forts to persuade her to undergo FNA ended in failure.

Most carcinomas associated with GD appear to be small, micro-papillary carcinomas [43]. Indeed, among the 336 carcinomas whose histologic type was shown in the previous studies reviewed by us (Table 1), most of them, 273 carcinomas, were papillary whereas no ATC was found. To the best of our knowledge, only 6 case reports, including the one presented here, of ATC associated with hyperthyroidism have ever been published [3, 4, 16, 17]. Among them, there was only one case report by Fujikawa *et al.* [4] that clearly showed association of GD and ATC. In our case, TSAb may have promoted the anaplastic transformation of the papillary carcinoma, as was also hypothesized by Fujikawa *et al.* [4]. While it has often been postulated that TSAb increases aggressiveness in well-differentiated thyroid cancer, whether ATC in GD is more aggressive or not and whether TSAb affects the behavior of ATC are unclear [1, 2, 4] because of their rare association.

The reported risk factors for ATC are age, gender, acute symptoms, larger tumor size, distant metastasis, and leukocytosis [15], which are important but not quite enough to establish suspicion of ATC at an early stage. Although there have been some case reports showing ATC producing granulocyte colony-stimulating factor (G-CSF) or parathyroid hormone-related protein (PTH-rp) [14, 45], neither higher G-CSF nor higher PTH-rp was found in our study. It is widely believed that multiple incidents of damage to the genome including p53 mutations lead to anaplastic transformation of differentiated thyroid cancer [14], but, unfortunately, genetic testing cannot be performed with ease and was not done in our study. Takano [46] has recently suggested that the remnants of fetal thyroid cells constitute a risk factor for anaplastic transformation, although they were also difficult to identify. Further studies are warranted to clarify risk factors for ATC, including whether TSAb or GD itself is a risk factor for anaplastic transformation.

Surgical treatment [2, 10, 11, 22, 43], or at least a low threshold for surgical referral [1, 2, 20, 43], is considered by many to be the most appropriate modality for thyroid nodules associated with GD, because there are no pre-operative investigations that can exclude malignancy with certainty in spite of the high risk of malignancy in those nodules and their aggressive behavior [13]. In addition, some clinical studies have found that complete removal of the primary lesion of ATC at an early stage has been associated with better prognosis [15]. Therefore, it might have been better to decide to perform thyroidectomy at the initial visit in this case, which might have rescued the patient.

In conclusion, our case is pathophysiologically interesting because it suggests that GD or TSAb may stimulate malignant transformation of differentiated carcinoma. It is also clinically important because it indicates that all thyroid nodules, particularly non-occult (>10 mm) cold nodules, associated with GD require careful and intensive management to detect malignancy because they are at higher risk of harboring malignancy.

References

1. Belfiore A, Russo D, Vigneri R, Filetti S (2001) Graves' disease, thyroid nodules and thyroid cancer. *Clin Endocrinol (Oxf)* 55: 711–718.
2. Stocker DJ, Burch HB (2003) Thyroid cancer yield in patients with Graves' disease. *Minerva Endocrinol* 28: 205–212.
3. Hayes FJ, Sheahan K, Heffernan A, McKenna TJ (1996) Aggressive thyroid cancer associated with toxic nodular goitre. *Eur J Endocrinol* 134: 366–370.
4. Fujikawa M, Okamura K, Sato K, Asano T, Yamasaki K, Hirata T, Ohta M, Mizokami T, Kuroda T, Fujishima M (1998) Anaplastic transformation of a papillary carcinoma of the thyroid in a patient with Graves' disease with varied activity of thyrotropin receptor antibodies. *Thyroid* 8: 53–58.
5. Behar R, Arganini M, Wu TC, McCormick M, Straus FH 2nd, DeGroot LJ, Kaplan EL (1986) Graves' disease and thyroid cancer. *Surgery* 100: 1121–1127.
6. Ozaki O, Ito K, Kobayashi K, Toshima K, Iwasaki H, Yashiro T (1990) Thyroid carcinoma in Graves' disease. *World J Surg* 14: 437–441.
7. Belfiore A, Garofalo MR, Giuffrida D, Runello F, Filetti S, Fiumara A, Ippolito O, Vigneri R (1990) Increased aggressiveness of thyroid carcinoma patients with Graves' disease. *J Clin Endocrinol Metab* 70: 830–835.
8. Pellegriti G, Belfiore A, Giuffrida D, Lupo L, Vigneri R (1998) Outcome of differentiated thyroid cancer in Graves' patients. *J Clin Endocrinol Metab* 83: 2805–2809.
9. Chao TC, Lin JD, Jeng LB, Chen MF (1999) Thyroid cancer with concurrent hyperthyroidism. *Arch Surg*

134: 130–134.
10. Kraimps JL, Bouin-Pineau MH, Mathonnet M, De Calan L, Ronceray J, Visset J, Marechaud R, Barbier J (2000) Multicentre study of thyroid nodules in patients with Graves' disease. *Br J Surg* 87: 1111–1113.
11. Mishra A, Mishra SK (2001) Thyroid nodules in Graves' disease: implications in an endemically iodine deficient area. *J Postgrad Med* 47: 244–247.
12. Gabriele R, Letizia C, Borghese M, De Toma G, Celi M, Izzo L, Cavallaro A (2003) Thyroid cancer in patients with hyperthyroidism. *Horm Res* 60: 79–83.
13. Kim WB, Han SM, Kim TY, Nam-Goong IS, Gong G, Lee HK, Hong SJ, Shong YK (2004) Ultrasonographic screening for detection of thyroid cancer in patients with Graves' disease. *Clin Endocrinol (Oxf)* 60: 719–725.
14. Sugitani I, Kasai N, Fujimoto Y, Yanagisawa A (2001) Prognostic factors and therapeutic strategy for anaplastic carcinoma of the thyroid. *World J Surg* 25: 617–622.
15. Kihara M, Miyauchi A, Yamauchi A, Yokomise H (2004) Prognostic factors of anaplastic thyroid carcinoma. *Surg Today* 34: 394–398.
16. Mangla JC, Rastogi GK, Pathak IC (1967) Anaplastic carcinoma of the thyroid complicating severe thyrotoxicosis. *J Indian Med Assoc* 49: 286, 291–292.
17. Oppenheim A, Miller M, Anderson GH Jr, Davis B, Slagle T (1983) Anaplastic thyroid cancer presenting with hyperthyroidism. *Am J Med* 75: 702–704.
18. Dobyns BM, Sheline GE, Workman JB, Tompkins EA, McConaley WM, Becker DV (1974) Malignant and benign neoplasms of the thyroid in patients treated for hyperthyroidism. *J Clin Endocrinol Metab* 38: 976–998.
19. Pacini F, Elisei R, Di Coscio GC, Anelli S, Macchia E, Concetti R, Miccoli P, Arganini M, Pinchera A (1988) Thyroid carcinoma in thyrotoxic patients treated by surgery. *J Endocrinol Invest* 11: 107–112.
20. Carnell NE, Valente WA (1998) Thyroid nodules in Graves' disease: classification, characterization, and response to treatment. *Thyroid* 8: 647–652.
21. Cantalamessa L, Baldini M, Orsatti A, Meroni L, Amodei V, Castagnone D (1999) Thyroid nodules in Graves' disease and the risk of thyroid carcinoma. *Arch Intern Med* 159: 1705–1708.
22. Lin CH, Chiang FY, Wang LF (2003) Prevalence of thyroid cancer in hyperthyroidism treated by surgery. *Kaohsiung J Med Sci* 19: 379–384.
23. Beahrs OH, Pemberton Jde J, Black BM (1951) Nodular goiter and malignant lesions of the thyroid gland. *J Clin Endocrinol Metab* 11: 1157–1165.
24. Sokal JE (1954) Incidence of malignancy in toxic and nontoxic nodular goiter. *JAMA* 154: 1321–1325.
25. Shapiro SJ, Friedman NB, Perzik SL, Catz B (1970) Incidence of thyroid carcinoma in Graves' disease. *Cancer* 26: 1261–1270.
26. Hancock BW, Bing RF, Dirmikis SM, Munro DS, Neal FE (1977) Thyroid carcinoma and concurrent hyperthyroidism: a study of ten patients. *Cancer* 39: 298–302.
27. Wahl RA, Goretzki P, Meybier H, Nitschke J, Linder M, Roher HD (1982) Coexistence of hyperthyroidism and thyroid cancer. *World J Surg* 6: 385–390.
28. Farbota LM, Calandra DB, Lawrence AM, Paloyan E (1985) Thyroid carcinoma in Graves' disease. *Surgery* 98: 1148–1153.
29. Rieger R, Pimpl W, Money S, Rettenbacher L, Galvan G (1989) Hyperthyroidism and concurrent thyroid malignancies. *Surgery* 106: 6–10.
30. Hales IB, McElduff A, Crummer P, Clifton-Bligh P, Delbridge L, Hoschl R, Poole A, Reeve TS, Wilmshurst E, Wiseman J (1992) Does Graves' disease or thyrotoxicosis affect the prognosis of thyroid carcinoma. *J Clin Endocrinol Metab* 75: 886–889.
31. Chou FF, Sheen-Chen SM, Chen YS, Chen MJ (1993) Hyperthyroidism and concurrent thyroid cancer. *Int Surg* 78: 343–346.
32. Terzioglu T, Tezelman S, Onaran Y, Tanakol R (1993) Concurrent hyperthyroidism and thyroid carcinoma. *Br J Surg* 80: 1301–1302.
33. Soh EY, Park CS (1993) Diagnostic approach to thyroid carcinoma in Graves' disease. *Yonsei Med J* 34: 191–194.
34. Kasuga Y, Sugenoya A, Kobayashi S, Masuda H, Iida F (1993) The outcome of patients with thyroid carcinoma and Graves' disease. *Surg Today* 23: 9–12.
35. Thakur S, Sharma AK, Agarwal A, Mishra SK, Bhatia E (1995) Carcinoma in Graves' disease. *J Assoc Physicians India* 43: 600–601.
36. Miccoli P, Vitti P, Rago T, Iacconi P, Bartalena L, Bogazzi F, Fiore E, Valeriano R, Chiovato L, Rocchi R, Pinchera A (1996) Surgical treatment of Graves' disease: subtotal or total thyroidectomy? *Surgery* 120: 1020–1024.
37. Pomorski L, Cywinski J, Rybinski K (1996) Cancer in hyperthyroidism. *Neoplasma* 43: 217–219.
38. Vaiana R, Cappelli C, Perini P, Pinelli D, Camoni G, Farfaglia R, Balzano R, Braga M (1999) Hyperthyroidism and concurrent thyroid cancer. *Tumori* 85: 247–252.
39. Ruggieri M, Scocchera F, Genderini M, Mascaro A, Luongo B, Paolini A (1999) Hyperthyroidism and concurrent thyroid carcinoma. *Eur Rev Med Pharmacol Sci* 3: 265–268.
40. Zanella E, Rulli F, Sianesi M, Sciacchitano S, Danese D, Pontecorvi A, Farinon AM (2001) Hyperthyroidism with concurrent thyroid cancer. *Ann Ital Chir* 72: 293–297.
41. Stocker DJ, Foster SS, Solomon BL, Shriver CD, Burch HB (2002) Thyroid cancer yield in patients with Graves' disease selected for surgery on the basis of

cold scintiscan defects. *Thyroid* 12: 305–311.
42. Gerenova J, Buysschaert M, de Burbure CY, Daumerie C (2003) Prevalence of thyroid cancer in Graves' disease: a retrospective study of a cohort of 103 patients treated surgically. *Eur J Intern Med* 14: 321–325.
43. Chao TC, Lin JD, Chen MF (2004) Surgical treatment of thyroid cancers with concurrent Graves disease. *Ann Surg Oncol* 11: 407–412.
44. Majima T, Doi K, Komatsu Y, Itoh H, Fukao A, Shigemoto M, Takagi C, Corners J, Mizuta N, Kato R, Nakao K (2005) Papillary thyroid carcinoma without metastases manifesting as an autonomously functioning thyroid nodule. *Endocr J* 52: 309–316.
45. Iwai H, Ohno Y, Aoki N (2004) Anaplastic thyroid carcinoma with humoral hypercalcemia of malignancy (HHM): an autopsy case report. *Endocr J* 51: 303–310.
46. Takano T (2004) Fetal cell carcinogenesis of the thyroid: a hypothesis for better understanding of gene expression profile and genomic alternation in thyroid carcinoma. *Endocr J* 51: 509–515.

Circ J 2005; **69:** 1412–1417

SOCS1/JAB Likely Mediates the Protective Effect of Cardiotrophin-1 Against Lipopolysaccharide-Induced Left Ventricular Dysfunction In Vivo

Keiji Tanimoto, MD; Yoshihiko Saito, MD; Ichiro Hamanaka, MD; Koichiro Kuwahara, MD; Masaki Harada, MD; Nobuki Takahashi, MD; Rika Kawakami, MD; Yasuaki Nakagawa, MD; Michio Nakanishi, MD; Yuichiro Adachi, PhD; Gotaro Shirakami, MD*; Kazuhiko Fukuda, MD*; Akihiko Yoshimura, PhD**; Kazuwa Nakao, MD

Background Suppressor of cytokine signaling 1 (SOCS1) is a negative regulator of cytokine signaling whose expression is induced in the rat heart by cardiotrophin-1 (CT-1). Sepsis-induced myocardial depression results from the expression of inducible nitric oxide synthase (iNOS) evoked by inflammatory cytokines.

Methods and Results The effect of CT-1 on lipopolysaccharide (LPS)-induced cardiac dysfunction was examined in a rat model of sepsis. In the absence of CT-1, LPS (1 mg/kg ip) elicited a reduction of systolic function and dilation of the ventricular cavity within 3–6 h after administration. These physiological effects were accompanied by increased ventricular phosphorylation of signal transducers and activators of transcription (STAT) 1 and STAT3, activation of nuclear factor-κB and expression of iNOS mRNA. Notably, administration of CT-1 (20 μg/kg iv) immediately prior to LPS significantly inhibited all of these LPS-induced changes. To determine whether SOCS1 expression in cardiomyocytes is sufficient to inhibit LPS- and cytokine-induced expression of iNOS mRNA, the effects of forced expression of SOCS1 in cultured neonatal cardiomyocytes were investigated using an adenovirus-mediated transfection system. Forced expression of SOCS1 significantly inhibited iNOS transcription induced by LPS, tumor necrosis factor-α or interferon-γ.

Conclusions CT-1-mediated expression of SOCS1 in cardiomyocytes may be a useful target for preventing sepsis-induced myocardial depression. (*Circ J* 2005; **69:** 1412–1417)

Key Words: Cardiotrophin-1; Lipopolysaccharide; Sepsis; SOCS1/JAB

Proinflammatory cytokines are involved in the pathogenesis of various heart diseases, such as septic shock, myocarditis, some cases of dilated cardiomyopathy, ischemic heart disease and cardiac hypertrophy[1–7] The effects of some cytokines, which act in an autocrine or paracrine manner, on the heart have been extensively studied. Contributing to the profound cardiocirculatory abnormalities in septic shock is myocardial depression, which some evidence suggests can be attributed to circulating inflammatory cytokines such as tumor necrosis factor (TNF)-α, interleukin (IL)-1β and interferon (IFN)-γ[8] These mediators activate nuclear factor (NF)-κB in cardiomyocytes, which in turn leads to upregulation of inducible nitric oxide synthase (iNOS) expression, resulting in acute left ventricular (LV) dysfunction caused by the negative inotropic effect of nitric oxide (NO)[9,10] Induction of iNOS in cardiomyocytes was likewise demonstrated in an animal model in which septic shock was produced by administration of lipopolysaccharide (LPS) or endotoxin derived from gram-negative bacterial membranes[11,12]

(Received March 29, 2005; revised manuscript received July 29, 2005; accepted August 11, 2005)

*Departments of Medicine and Clinical Science, *Anesthesia, Kyoto University Graduate School of Medicine, Kyoto and **Division of Molecular and Cellular Immunology, Medical Institute of Bioregulation, Kyushu University, Fukuoka, Japan*

Mailing address: Yoshihiko Saito, MD, First Department of Internal Medicine, Nara Medical University, 840 Shijo-cho, Kashihara, Nara 630-0813, Japan. E-mail: yssaito@naramed-u.ac.jp

The suppressor of cytokine signaling (SOCS) family is a recently identified group of proteins (SOCS1 to SOCS7 and cytokine-inducible SH2-containing protein) that function in a negative feedback loop that regulates signaling mediated by cytokine receptors via the Janus kinase (JAK)-signal transducers and activators of transcription (STAT) pathway[13–15] SOCS proteins appear to use several mechanisms to inhibit cytokine signaling[16] For instance, SOCS1/JAB (JAK binding protein), which is activated by phosphorylated STAT1 and STAT3, binds directly to the kinase domain of JAK1 and JAK2, thereby inhibiting STAT signal transduction. SOCS1 also suppresses LPS signal transduction through one of the Toll-like receptors (TLRs), TLR4, via which LPS triggers innate immune responses[17,18] In addition, SOCS1 reportedly inhibits signaling by mediators other than JAK-STAT, including TNF-α, insulin and Vav[19–22] Although the SOCS1 target molecule in TLR4 signaling has not yet been identified, collectively the available data suggest that induction of SOCS1 could play a protective role during septic shock by modulating the cardiovascular response.

We recently reported that intravenous injection of cardiotrophin-1 (CT-1), a cytokine in the IL-6 family, into Wistar rats induces phosphorylation of STAT3 and expression of SOCS1 and SOCS3 in various tissues[23] In addition, injection of CT-1 induced resistance to a second CT-1 injection; that is, it lead to attenuation of the STAT3 phosphorylation, iNOS mRNA expression and blood pressure reduction seen otherwise. In the present report we show that induction of

SOCS1 by CT-1 in vivo prevents LPS-induced LV dysfunction in association with significant reductions in the activation of STAT1, STAT3 and NF-κB.

Methods

Animals

Male Wistar rats (250–270 g, Shimizu Experiment, Tokyo) were housed in a light- and temperature-controlled room, where they received rat chow and water ad libitum. All experimental procedures were carried out in accordance with Kyoto University standards for animal care.

Reagents

Rat recombinant CT-1 was prepared using a glutathione S-transferase fusion system described previously[24] The purity of the CT-1 was verified by sodium dodecyl sulfate-polyacrylamide gel electrophoresis and quantified by colorimetric assay (Bio-Rad Laboratories, Hercules, CA, USA).

LPS-Induced Sepsis Model

Rats were intraperitoneally injected with 1 mg/kg body weight of LPS from Salmonella typhimurium (Sigma, St Louis, MO, USA).

Administration of CT-1

CT-1 at a concentration of 20 μg/kg body weight in 100 μl of phosphate-buffered saline (PBS) was injected via an intravenous catheter immediately before LPS administration. Control rats received an equal volume of PBS alone.

Echocardiographic Studies

After placing rats under light isoflurane (0.5%) anesthesia, changes of LV function 0, 1, 3 and 6 h after LPS injection were examined by transthoracic echocardiography (Hewlett-Packard) using a 7.5-MHz probe. The end-diastolic diameter (EDD) and end-systolic diameter (ESD) were measured from the M-mode tracings according to the American Society for Echocardiology leading-edge method. LV fractional shortening (FS) was calculated as follows: LV FS (%) = [(EDD − ESD)/EDD] × 100.

Protein Extraction and Western Blot Analysis

Protein extraction and western blotting were carried out as described previously[25] For detection of STAT1, STAT3 and their phosphorylated forms, membranes were incubated first with the appropriate primary antibody (New England Biolabs, Inc, Beverly, MA, USA) and then with peroxidase-conjugated goat anti-rabbit IgG antibody (DACO, Tokyo, Japan). Bands were visualized by chemiluminescence detection (NEN Life Science Products Inc, Boston, MA, USA).

RNA Extraction and Northern Blot Analysis

At selected times after LPS administration, rats were anesthetized with 50 mg/kg pentobarbital and then killed. The left ventricles were removed and homogenized in TRIzol Reagent (GIBCO/BRL, Life technologies, Inc), after which total RNA was isolated according to the manufacturer's instructions. Samples (20 μg) of total RNA were then separated, transferred to Biodyne membranes (Pall Corp, Glen Cove, NY, USA), and hybridized with ^{32}P-labeled probes as previously described[26]

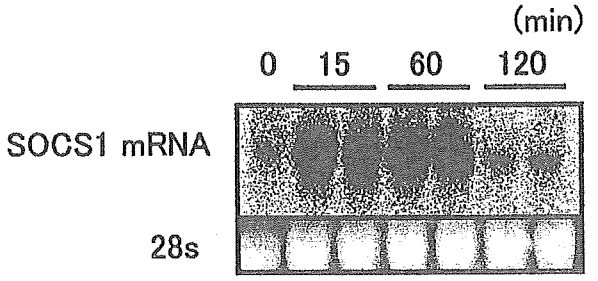

Fig 1. Northern blot analysis of suppressor of cytokine signaling 1 (SOCS1) mRNA expression in rat hearts harvested at the indicated times after intravenous injection of 20 μg/kg cardiotrophin-1.

Nuclear Protein Extract and Electrophoretic Mobility Shift Assay

Activation of NF-κB was assessed in nuclear extracts prepared from frozen myocardial tissue[27] using an electrophoretic mobility shift assay (EMSA). An NF-κB consensus oligonucleotide probe (5'-AGTTGAGGGGACTTTCCCAGGC-3') was end-labeled with γ-^{32}P ATP (Amersham Pharmacia Biotech, Piscataway, NJ, USA) using T4 polynucleotide kinase. DNA-protein binding reactions were carried out in a 20-μl final volume of reaction buffer containing 10 mmol/L Tris-HCl (pH 7.5), 50 mmol/L NaCl, 0.5 mmol/L dithiothreitol, 10% glycerol, 1 mmol/L $MgCl_2$, 0.5 mmol/L EDTA, and 1 μg of poly (dI-dC). After preincubating 15 μg of nuclear protein in reaction buffer for 10 min on ice, the radiolabeled DNA probe was added and incubated for an additional 30 min at room temperature. The reaction mixture was then loaded onto a 4% polyacrylamide gel and electrophoresed at 250 V in 0.5 × Tris-borate EDTA buffer. The gels were then dried using a Gel-drier and radiographed.

Cell Culture and Transfections

Neonatal rat ventricular myocytes were prepared on a Percoll gradient as previously described[26] The system used for introducing cDNA into the adenoviral genome has also been described previously[28] The recombinant virus AxLNLSOCS1 was a gift from Dr Hanakawa (Ehime University, Japan); AxCANCre and AxCALacZ were gifts from Dr Saito (Tokyo University, Japan). One day after plating, ventricular myocytes were infected with adenovirus at a multiplicity of infection of 5 particles/cell for 24 h in Dulbecco's modified Eagle medium supplemented with 10% fetal calf serum. The cells were then cultured in serum-free medium for an additional 24 h. Using the level of lacZ expression as a reporter, we determined that with this protocol the efficiency of expression in cultured ventricular myocytes was consistently more than 90%.

Statistical Analysis

All results are expressed as means ± SEM. Comparisons between 2 groups were made using unpaired Student's t-tests. ANOVA with post hoc Fisher's tests was used to determine significant differences among 3 or 4 groups. Values of $p<0.05$ were considered significant.

Results

CT-1 Treatment Upregulates SOCS1 mRNA Expression in the Heart

As we previously reported[23] intravenous injection of

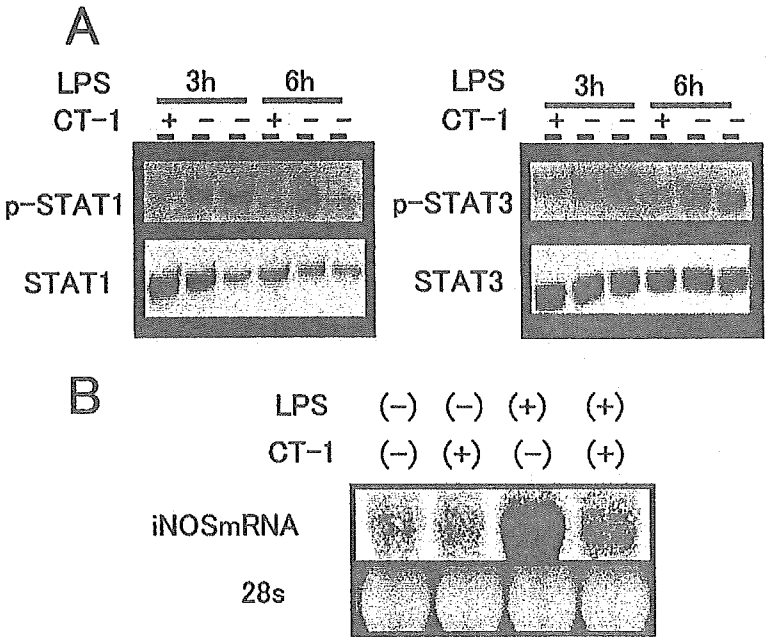

Fig 2. (A) Western blot analysis of p signal transducers and activators of transcription (STAT) 1, STAT1, pSTAT3 and STAT3 expression in whole cell lysates prepared from rat hearts harvested 3 h and 6 h after administration of 1 mg/kg lipopolysaccharide (LPS) with or without 20 μg/kg cardiotrophin-1 (CT-1). (B) Representative northern blot analysis of inducible nitric oxide synthase (iNOS) mRNA expression in hearts harvested 6 h after administration of LPS with or without CT-1.

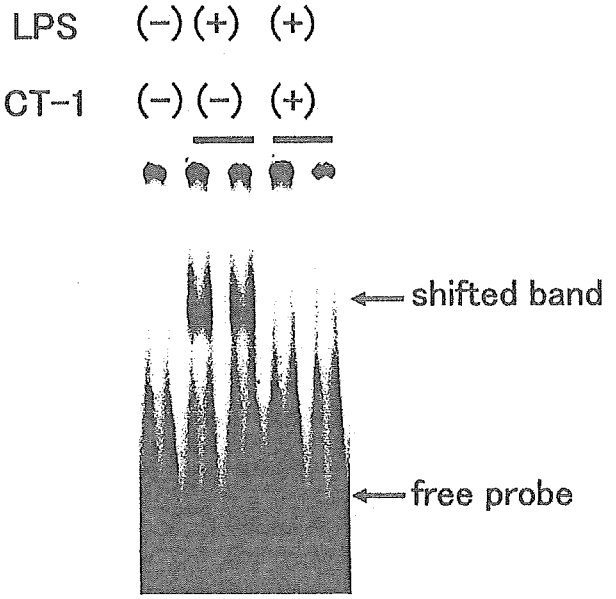

Fig 3. Electrophoretic mobility shift assay (EMSA) showing nuclear factor-κB activation in nuclear extracts prepared from rat hearts harvested 6 h after administration of lipopolysaccharide (LPS) with or without cardiotrophin-1 (CT-1).

20 μg/kg body weight of CT-1 induced prompt, transient expression of SOCS1 mRNA in the heart (Fig 1). Prior to CT-1 injection only low levels of SOCS1 mRNA were detectable. Administration of CT-1 induced a dramatic increase in the expression of SOCS1 mRNA that peaked within 15–60 min and then returned to baseline within 120 min.

Pretreatment With CT-1 Diminishes Phosphorylation of STAT1 and STAT3 and Expression of iNOS mRNA

To investigate the pharmacological effect of CT-1-induced SOCS expression, rats were administered a sublethal dose (1 mg/kg body weight ip) of LPS, with or without CT-1 (20 μg/kg body weight iv) pretreatment, after which LPS-induced STAT1 and STAT3 phosphorylation was evaluated. Consistent with earlier findings,[9] LPS induced phosphorylation of both STAT1 and STAT3 within 3 h and 6 h, respectively (Fig 2A). This effect was strongly inhibited by pretreatment with CT-1 (Fig 2A), as was LPS-induced expression of iNOS mRNA (Fig 2B).

CT-1 Pretreatment Inhibits NF-κB Activation in the Heart

Activation of NF-κB plays a critical role in mediating LPS-induced iNOS expression,[10] so we used EMSA to assess NF-κB activation in nuclear extracts from the hearts of rats administered LPS with or without CT-1 pretreatment. As shown in Fig 3, no basal activation of NF-κB was detected in extracts from control hearts, but extracts from hearts harvested 6 h after administration of LPS showed a clearly detectable band shift, indicating activation of NF-κB. That activation was completely blocked by pretreatment with CT-1.

CT-1 Pretreatment Protects LPS-Induced LV Dysfunction

As mentioned before, pretreating rats with CT-1 inhibits cardiac expression of iNOS. In sepsis, elevation of iNOS causes NO-mediated vasorelaxation and myocardial depression, which is characterized by LV dysfunction.[9,10] Moreover, examination of the relationship between endotoxin and the typical cardiovascular manifestations of sepsis has shown that a reduction in ejection fraction is a useful measure of ventricular performance during sepsis and septic shock.[8] In the present study, echocardiographic examination of LV function revealed that LPS (1 mg/kg body weight ip) causes a reduction of systolic function accompanied by dilation of the ventricular cavity within 3–6 h, and that this myocardial depression was significantly diminished by pretreatment with CT-1 (Fig 4A,B). Echocardiographic examination of LV function for 6 h after administration of CT-1 alone revealed it to have no positive or negative inotropic effects (data not shown). This is consistent with our recent findings that CT-1 has no effect on the maximum rate of rise (dP/dT) in LV developed pressure and perfusion

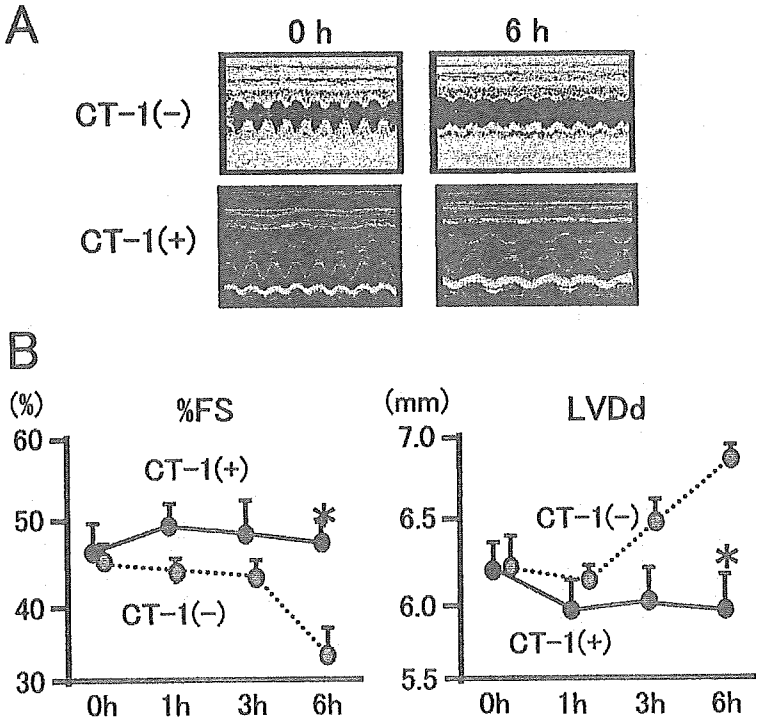

Fig 4. (A) Representative transthoracic echocardiographs obtained before (0 h) and after (6 h) administration of lipopolysaccharide (LPS) with or without cardiotrophin-1 (CT-1 (+) and CT-1 (–), respectively). (B) Changes in the fractional shortening (%FS) (Left panel) and left ventricular diastolic diameter (LVDd) (Right panel) at the indicated times after LPS administration with (solid line) or without (dotted line) CT-1 (n=5 in each group).

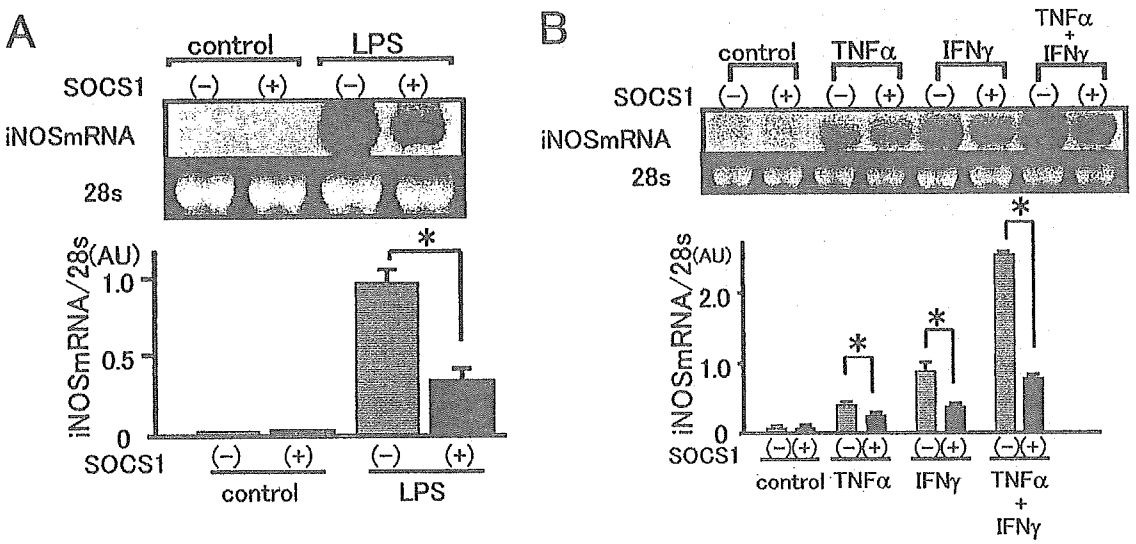

Fig 5. (A) Representative northern blot analysis of inducible nitric oxide synthase (iNOS) mRNA expression in cardiac myocytes transfected with LacZ (–) or suppressor of cytokine signaling 1 (SOCS1) (+) and then exposed for 6 h to 50 μg/ml lipopolysaccharide (LPS) in phosphate-buffered saline (PBS) (LPS) or to the same volume of PBS alone (control). (B) Transfectants were exposed for 6 h to 400 IU/ml tumor necrosis factor-α (TNF-α) and/or 100 IU/ml interferon-γ (IFN-γ) in fetal calf serum (–) medium. In each panel, the bar graphs show the relative iNOS mRNA levels, which were quantified from the optical density of the respective iNOS mRNA bands using NIH image software and normalized to the 28S bands. Relative iNOS mRNA levels in myocytes infected with Ad.LacZ and treated with LPS (a) or IFN-γ (b) were assigned a value of 1.0. The data are the means ± SEM from 2 independent experiments carried out in triplicate (See text for abbreviations).

pressure in the isolated perfused rat heart[30] and confirms that the inhibitory effect of CT-1 on LPS-induced LV dysfunction is indirect.

Adenovirus-Mediated Expression of SOCS1 Inhibits LPS, TNF-α and IFN-γ-Induced Expression of iNOS mRNA in Cardiomyocytes

We hypothesized that the protective effect of CT-1 against LPS-induced STAT phosphorylation and iNOS expression reflects its ability to induce SOCS expression in cardiomyocytes. To test that hypothesis, we first examined the effects of forced expression of SOCS1 in cultured neonatal cardiomyocytes using an adenovirus-mediated transfection system. In cells transfected with mock vector, LPS markedly increased expression of iNOS mRNA, even in the absence of macrophages or T lymphocytes (Fig 5A).

This effect was significantly inhibited by forced expression of SOCS1. In addition, to rule out the possibility that the observed inhibitory effect of SOCS1 is specific to LPS signaling, we examined the effect of SOCS1 on expression of iNOS mRNA induced by TNF-α and IFN-γ, which are both elevated in the circulation in cases of septic shock[8] Fig 5B shows that transfection of SOCS1 inhibited TNF-α- and IFN-γ-induced expression iNOS mRNA by 41.2% ($p<0.01$) and 67.2% ($p<0.01$), respectively, and completely blocked the synergistic induction of iNOS expression otherwise seen when the 2 cytokines were given together.

Discussion

We previously showed that pretreatment with CT-1 inhibits subsequent CT-1-induced STAT3 activation and iNOS mRNA expression in the lung[23] In the same study, we also found that forced expression of SOCS1 inhibits CT-1-induced STAT3 activation in 293 cells. With that in mind, we hypothesized that CT-1-induced SOCS1 expression in the heart might exert a protective effect during the pathogenesis of sepsis, in which cytokines play key roles. In support of that hypothesis, we have shown here that CT-1 prevents LPS-induced acute LV dysfunction and inhibits signaling transduced via JAK/STAT, NF-κB and iNOS in the heart, and that forced expression of SOCS1 attenuates iNOS mRNA expression induced by LPS, TNF-α, and IFN-γ in cultured cardiomyocytes. Thus the mechanism by which CT-1 downregulates LPS-induced iNOS expression and LV dysfunction appears to involve an upregulation of cardiac SOCS1 activity. Our findings further suggest that CT-1-induced SOCS1 activity in the heart is not only involved in a classical negative feedback loop; CT-1 also confers cross-resistance to other groups of cytokines produced by LPS challenge in vivo. This is consistent with recent in vitro evidence that upregulation of SOCS attenuates signaling by a variety of cytokines and hormones[31–33]

LPS is a major cause of the clinical manifestations of septic shock. LPS-activated cells elicit many of their pathological effects by releasing second mediators, such as proinflammatory cytokines and reactive oxygen and nitrogen species. For instance, in the progression of sepsis into septic shock, there is a rapid increase in the circulating levels of TNF-α, IFN-γ, IL-1β and IL-6, and induction of iNOS by these cytokines is at least partly responsible for the cardiovascular dysfunction characteristic of septic shock. Regulation of iNOS activity is mainly transcriptional; the binding of STAT1 and NF-κB to their consensus sequences in the iNOS promoter appears to be required for full activation of the enzyme[34–36] Moreover, it was recently reported that the JAK2/STAT3 pathway mediates IL-6-induced iNOS activation, which in turn diminishes contractility in adult ventricular myocytes[37] Like the present findings, these results implicate JAK-STAT signaling and NF-κB activation in the progression of cytokine-induced LV dysfunction.

Our in vitro data indicate that forced expression of SOCS1 in cardiomyocytes inhibits expression of iNOS mRNA induced by LPS, IFN-γ and TNF-α, which is consistent with earlier findings that SOCS1 negatively regulates LPS signal transduction[17,18] The inhibition of IFN-γ signaling by SOCS1 likely reflects its ability to directly bind to JAK. Unlike IFN-γ, however, TNF-α does not primarily utilize the JAK-STAT pathway, and the mechanism of SOCS1's activity is less clear in this case. Still, the present findings likely reflect altered signal transduction within cardiomyocytes and are consistent with earlier work suggesting that SOCS1 inhibits both TNF-α-induced iNOS expression and NO-dependent cell death in pancreatic β cells[20]

Also unclear is the relative contribution made by SOCS1 to the total effect of CT-1 on myocardial function. This is because CT-1 also induces SOCS3, a related protein, and activates mitogen-activated protein kinase and the phosphatidylinositol 3-OH kinase pathway via a gp130-coupled receptor[23,38,39]

Volume resuscitation combined with administration of vasopressors, such as dopamine and noradrenaline, remains the standard care in septic shock. Unfortunately, the reduction in myocardial contractility is often resistant to β-adrenergic stimulation; it is unpreventable in those cases. It is therefore noteworthy that induction of SOCS1 in heart prevents LPS-induced LV dysfunction and thus suggests a possible therapeutic approach to this problem.

Acknowledgments

This work was supported in part by research grants from the Japanese Ministry of Education, Science and Culture, the Japanese Ministry of Health and Welfare, and the Research for the Future program of the Japan Society for the Promotion of Science (JSPS-RFTF96I00204 and 98L00801), and by grants from the Japanese Cardiovascular Research Foundation, Uehara Memorial Foundation and Smoking Research Foundation.

We thank Dr Hanakawa (Ehime University, Japan), Dr Saito (Tokyo University), Makoto Mukai and Kana Okamura for their assistance with this work.

References

1. Matsumori A, Yamada T, Suzuki H, Matoba Y, Sasayama S. Increased circulating cytokines in patients with myocarditis and cardiomyopathy. *Br Heart J* 1994; **72:** 561–566.
2. Torre Amione G, Kapadia S, Lee J, Durand J-B, Bies RD, Young JB, et al. Tumor necrosis factor-alpha and tumor necrosis factor receptors in the failing human heart. *Circulation* 1996; **93:** 704–711.
3. Herskowitz A, Choi S, Ansari AA, Wesselingh S. Cytokine mRNA expression in postischemic/reperfused myocardium. *Am J Pathol* 1995; **146:** 419–428.
4. Habib FM, Springall DR, Davies GJ, Oakley CM, Yacoub MH, Polak JM. Tumor necrosis factor and inducible nitric oxide synthase in dilated cardiomyopathy. *Lancet* 1996; **347:** 1151–1155.
5. Shioi T, Matsumori A, Kihara Y, Inoko M, Ono K, Iwanaga Y, et al. Increased expression of interleukin-1 beta and monocyte chemotactic and activating factor/monocyte chemoattractant protein-1 in the hypertrophied and failing heart with pressure overload. *Circ Res* 1997; **81:** 664–671.
6. Funayama H, Ishikawa S, Kubo N, Katayama T, Yasu T, Saito M, et al. Increases in interleukin-6 and metalloproteinase-9 in the infarct-related coronary artery of acute myocardial infarction. *Circ J* 2004; **68:** 451–454.
7. Tanaka T, Nakamura Y, Nasuno A, Mezaki T, Higuchi K, Fukunaga H, et al. Plasma concentrations of monocyte chemoattractant protein-1 (MCP-1) and neopterin in the coronary circulation of patients with coronary artery disease. *Circ J* 2004; **68:** 114–120.
8. Parrillo JE. Pathogenetic mechanisms of septic shock. *N Engl J Med* 1993; **328:** 1471–1477.
9. Ullrich R, Scherrer-Crosbie M, Bloch KD, Ichinose F, Nakajima H, Picard MH, et al. Congenital deficiency of nitric oxide synthase 2 protects against endotoxin-induced myocardial dysfunction in mice. *Circulation* 2000; **102:** 1440–1446.
10. Liu SF, Ye X, Malik AB. In vivo inhibition of nuclear factor-kappa B activation prevents inducible nitric oxide synthase expression and systemic hypotension in a rat model of septic shock. *J Immunol* 1997; **159:** 3976–3983.
11. Stein B, Frank P, Schmitz W, Scholz H, Thoenes M. Endotoxin and cytokines induce direct cardiodepressive effects in mammalian cardiomyocytes via induction of nitric oxide synthase. *J Mol Cell Cardiol* 1996; **28:** 1631–1639.
12. Frantz S, Kobzik L, Kim YD, Fukazawa R, Medzhitov R, Lee RT, et al. Toll4 (TLR4) expression in cardiac myocytes in normal and failing myocardium. *J Clin Invest* 1999; **104:** 271–280.
13. Endo TA, Masuhara M, Yokouchi M, Suzuki R, Sakamoto H, Mitsui

K, et al. A new protein containing an SH2 domain that inhibits JAK kinases. *Nature* 1997; **387:** 921–924.
14. Starr R, Willson TA, Viney EM, Murray LJ, Rayner JR, Jenkins BJ, et al. A family of cytokine-inducible inhibitors of signalling. *Nature* 1997; **387:** 917–921.
15. Naka T, Narazaki M, Hirata M, Matsumoto T, Minamoto S, Aono A, et al. Structure and function of a new STAT-induced STAT inhibitor. *Nature* 1997; **387:** 924–929.
16. Yasukawa H, Sasaki A, Yoshimura A. Negative regulation of cytokine signaling pathways. *Annu Rev Immunol* 2000; **18:** 143–164.
17. Nakagawa R, Naka T, Tsutsui H, Fujimoto M, Kimura A, Abe T, et al. SOCS-1 participates in negative regulation of LPS responses. *Immunity* 2002; **17:** 677–687.
18. Kinjyo I, Hanada T, Inagaki-Ohara K, Mori H, Aki D, Ohishi M, et al. SOCS1/JAB is a negative regulator of LPS-induced macrophage activation. *Immunity* 2002; **17:** 583–591.
19. Morita Y, Naka T, Kawazoe Y, Fujimoto M, Narazaki M, Nakagawa R, et al. Signals transducers and activators of transcription (STAT)-induced STAT inhibitor-1 (SSI-1)/suppressor of cytokine signaling-1 (SOCS-1) suppresses tumor necrosis factor alpha-induced cell death in fibroblasts. *Proc Natl Acad Sci USA* 2000; **97:** 5405–5410.
20. Chong MM, Thomas HE, Kay TW. Suppressor of cytokine signaling-1 regulates the sensitivity of pancreatic beta cells to tumor necrosis factor. *J Biol Chem* 2002; **277:** 27945–27952.
21. Kawazoe Y, Naka T, Fujimoto M, Kohzaki H, Morita Y, Narazaki M, et al. Signal transducer and activator of transcription (STAT)-induced STAT inhibitor 1 (SSI-1)/suppressor of cytokine signaling 1 (SOCS1) inhibits insulin signal transduction pathway through modulating insulin receptor substrate 1 (IRS-1) phosphorylation. *J Exp Med* 2001; **193:** 263–269.
22. De Sepulveda P, Ilangumaran S, Rottapel R. Suppressor of cytokine signaling-1 inhibits VAV function through protein degradation. *J Biol Chem* 2000; **275:** 14005–14008.
23. Hamanaka I, Saito Y, Yasukawa H, Kishimoto I, Kuwahara K, Miyamoto Y, et al. Induction of JAB/SOCS-1/SSI-1 and CIS3/SOCS-3/SSI-3 is involved in gp130 resistance in cardiovascular system in rat treated with cardiotrophin-1 in vivo. *Circ Res* 2001; **88:** 727–732.
24. Ishikawa M, Saito Y, Miyamoto Y, Kuwahara K, Ogawa E, Nakagawa O, et al. cDNA cloning of rat cardiotrophin-1 (CT-1): augmented expression of CT-1 gene in ventricle of genetically hypertensive rats. *Biochem Biophys Res Commun* 1996; **219:** 377–381.
25. Kuwahara K, Saito Y, Harada M, Ishikawa M, Ogawa E, Miyamoto Y, et al. Involvement of cardiotrophin-1 in cardiac myocyte-nonmyocyte interactions during hypertrophy of rat cardiac myocytes in vitro. *Circulation* 1999; **100:** 1116–1124.
26. Nakagawa O, Ogawa Y, Itoh H, Suga S, Komatsu Y, Kishimoto I, et al. Rapid transcriptional activation and early mRNA turnover of brain natriuretic peptide in cardiocyte hypertrophy. Evidence for brain natriuretic peptide as an "emergency" cardiac hormone against ventricular overload. *J Clin Invest* 1995; **96:** 1280–1287.
27. Izumi T, Saito Y, Kishimoto I, Harada M, Kuwahara K, Hamanaka I, et al. Blockade of the natriuretic peptide receptor guanylyl cyclase-A inhibits NF-kappaB activation and alleviates myocardial ischemia/reperfusion injury. *J Clin Invest* 2001; **108:** 203–213.
28. Hanakawa Y, Amagai M, Shirakata Y, Sayama K, Hashimoto K. Different effects of dominant negative mutants of desmocollin and desmoglein on the cell-cell adhesion of keratinocytes. *J Cell Sci* 2000; **113:** 1803–1811.
29. Cowan DB, Poutias DN, Del Nido PJ, McGowan FX Jr. CD14-independent activation of cardiomyocyte signal transduction by bacterial endotoxin. *Am J Physiol Heart Circ Physiol* 2000; **279:** H619–H629.
30. Hamanaka I, Saito Y, Nishikimi T, Magaribuchi T, Kamitani S, Kuwahara K, et al. Effects of cardiotrophin-1 on hemodynamics and endocrine function of the heart. *Am J Physiol Heart Circ Physiol* 2000; **279:** H388–H396.
31. Senn JJ, Klover PJ, Nowak IA, Zimmers TA, Koniaris LG, Furlanetto RW, et al. Suppressor of cytokine signaling-3 (SOCS-3), a potential mediator of interleukin-6-dependent insulin resistance in hepatocytes. *J Biol Chem* 2003; **278:** 13740–13746.
32. Leung KC, Doyle N, Ballesteros M, Sjogren K, Watts CK, Low TH, et al. Estrogen inhibits GH signaling by suppressing GH-induced JAK2 phosphorylation, an effect mediated by SOCS-2. *Proc Natl Acad Sci USA* 2003; **100:** 1016–1021.
33. Karlsen AE, Ronn SG, Lindberg K, Johannesen J, Galsgaard ED, Pociot F, et al. Suppressor of cytokine signaling 3 (SOCS-3) protects beta -cells against interleukin-1beta- and interferon-gamma -mediated toxicity. *Proc Natl Acad Sci USA* 2001; **98:** 12191–12196.
34. Ganster RW, Taylor BS, Shao L, Geller DA. Complex regulation of human inducible nitric oxide synthase gene transcription by Stat 1 and NF-kappa B. *Proc Natl Acad Sci USA* 2001; **98:** 8638–8643.
35. Samardzic T, Jankovic V, Stosic-Grujicic S, Trajkovic V. STAT1 is required for iNOS activation, but not IL-6 production in murine fibroblasts. *Cytokine* 2001; **13:** 179–182.
36. Gao J, Morrison DC, Parmely TJ, Russell SW, Murphy WJ. An interferon-gamma-activated site (GAS) is necessary for full expression of the mouse iNOS gene in response to interferon-gamma and lipopolysaccharide. *J Biol Chem* 1997; **272:** 1226–1230.
37. Yu X, Kennedy RH, Liu SJ. JAK2/STAT3, not ERK1/2, mediates interleukin-6-induced activation of inducible nitric-oxide synthase and decrease in contractility of adult ventricular myocytes. *J Biol Chem* 2002; **278:** 16304–16309.
38. Wollert KC, Chien KR. Cardiotrophin-1 and the role of gp130-dependent signaling pathways in cardiac growth and development. *J Mol Med* 1997; **75:** 492–501.
39. Kuwahara K, Saito Y, Kishimoto I, Miyamoto Y, Harada M, Ogawa E, et al. Cardiotrophin-1 phosphorylates akt and BAD, and prolongs cell survival via a PI3K-dependent pathway in cardiac myocytes. *J Mol Cell Cardiol* 2000; **32:** 1385–1394.

Available online at www.sciencedirect.com

SCIENCE DIRECT®

European Journal of Pharmacology 508 (2005) 255–265

ELSEVIER

ejp

www.elsevier.com/locate/ejphar

Therapeutic potential of thiazolidinediones in activation of peroxisome proliferator-activated receptor γ for monocyte recruitment and endothelial regeneration

Tokuji Tanaka[1], Yasutomo Fukunaga[1], Hiroshi Itoh*, Kentaro Doi, Jun Yamashita, Tae-Hwa Chun, Mayumi Inoue, Ken Masatsugu, Takatoshi Saito, Naoki Sawada, Satsuki Sakaguchi, Hiroshi Arai, Kazuwa Nakao

Department of Medicine and Clinical Science, Kyoto University Graduate School of Medicine, 54 Shogoin Kawahara-cho, Sakyo-ku, Kyoto 606-8507, Japan

Received 8 July 2004; received in revised form 18 October 2004; accepted 28 October 2004
Available online 30 December 2004

Abstract

Thiazolidinediones, a new class of antidiabetic drugs that increase insulin sensitivity, have been shown to be ligands for peroxisome proliferator-activated receptor γ (PPARγ). Recent studies demonstrating that PPARγ occurs in macrophages have focused attention on its role in macrophage functions. In this study, we investigated the effect of thiazolidinediones on monocyte proliferation and migration in vitro and the mechanisms involved. In addition, we examined the therapeutic potentials of thiazolidinediones for injured atherosclerotic lesions. Troglitazone and pioglitazone, the two thiazolidinediones, as well as 15-deoxy-Δ12,14-prostaglandin J2 inhibited in a dose-dependent manner the serum-induced proliferation of THP-1 (human monocytic leukemia cells) and of U937 (human monoblastic leukemia cells), which permanently express PPARγ. These ligands for PPARγ also significantly inhibited migration of THP-1 induced by monocyte chemoattractant protein-1 (MCP-1). Troglitazone and 15-deoxy-Δ12,14-prostaglandin J2 significantly suppressed the mRNA expression of the MCP family-specific receptor CCR2 (chemokine CCR2 receptor) in THP-1 at the transcriptional level. Furthermore, troglitazone significantly inhibited MCP-1 binding to THP-1. Oral administration of troglitazone to Watanabe heritable hyperlipidemic (WHHL) rabbits after balloon injury suppressed acute recruitment of monocytes/macrophages and accelerated re-endothelialization. These results suggest that thiazolidinediones have therapeutic potential for the treatment of diabetic vascular complications.

Keywords: Thiazolidinedione; PPARγ; MCP-1; CCR2; Macrophage; Insulin resistance

1. Introduction

Recruitment of circulating monocytes and their proliferation and differentiation into macrophages are not only the central events for initiation and progression of atherosclerosis, but have also been recently recognized as crucial pathogenic events in both diabetic micro- and macroangiopathy. Monocyte chemoattractant protein (MCP)-1 is a member of the C-C branch (or β) of the chemokine family and a potent monocyte and lymphocyte chemoattractant, which is expressed abundantly in atherosclerosic lesions (Nelken et al., 1991). MCP-1 initiates signal transduction through binding to the chemokine CCR2 receptor (CCR2) (Charo et al., 1994). In a study of CCR2 knockout mice, markedly fewer macrophages were present in the aorta of CCR2−/−, apoE−/− double knockout mice than in that of apoE−/− mice (Boring et al., 1998). Moreover, an independent study demonstrated that MCP-1−/− mice, when crossed with LDL receptor−/− mice, had smaller lesions and a significant reduction of macrophages in the lesions (Gu et al., 1998). These findings indicate the direct role of MCP-1 and CCR2 in monocyte recruitment and atherosclerosis.

* Corresponding author. Tel.: +81 75 751 3170; fax: +81 75 771 9452.
E-mail address: hiito@kuhp.kyoto-u.ac.jp (H. Itoh).
[1] These two authors contributed equally to this work.

0014-2999/$ - see front matter © 2004 Elsevier B.V. All rights reserved.
doi:10.1016/j.ejphar.2004.10.056

Thiazolidinediones are a new class of antidiabetic agents that increase sensitivity to insulin (Nolan et al., 1994). Insulin resistance has been attracting attention as the common casual factor not only for diabetes mellitus but also for hypertension, hyperlipidemia and obesity, all of which are risk factors for atherosclerosis (DeFronzo and Ferrannini, 1991). Recently, thiazolidinediones have been shown to be the ligands for peroxisome proliferator-activated receptor γ (PPARγ), which is a member of the nuclear receptor superfamily of ligand-activated transcription factors and has been identified as the functional receptor in antidiabetic action of thiazolidinediones (Lehmann et al., 1995).

PPARγ and the retinoid X receptor contain a heterodimer to bind regulatory elements in the promoter region of a number of adipocyte-specific genes and stimulate transcription (Tontonoz et al., 1994). In a previous study, we cloned rat PPARγ and detected down-regulation of PPARγ mRNA by several cytokines (Tanaka et al., 1999). Recent studies have demonstrated that PPARγ is expressed in cells of monocyte/macrophage lineage (Ricote et al., 1998; Tontonoz et al., 1998), and that oxidized low density lipoprotein (oxLDL), which plays a central role in atherogenesis, can regulate PPARγ-dependent gene transcription (Nagy et al., 1998). We recently reported that oxLDL potentiates, through the activation of PPARγ, the expression of vascular endothelial growth factor (VEGF) in human endothelial cells and in monocytes/macrophages (Inoue et al., 2001). Another study demonstrated that the administration of troglitazone, one of the thiazolidinediones, to Watanabe heritable hyperlipidemia (WHHL) rabbits and high fat-fed low density lipoprotein receptor or apo E knockout mice inhibits progression of atherosclerosis (Shiomi et al., 1999; Chen et al., 2001; Collins et al., 2001). All of these studies indicate the significance of PPARγ in monocyte and macrophage functions and atherogenesis.

The objective of the study presented here was to determine the effect of thiazolidinediones on the migration and proliferation of monocytes/macrophages and to investigate the molecular mechanism of the effect of thiazolidinediones on MCP-1-induced monocyte migration, with the focus on the expression of CCR2. Furthermore, we used WHHL atherosclerotic rabbits for an in vivo investigation of the therapeutic potentials of thiazolidinediones for acute monocyte recruitment and infiltration as well as for endothelial regeneration after acute vascular injury.

2. Materials and methods

2.1. Cell culture

THP-1 (human monocytic leukemia cells) and U937 (human monoblastic leukemia cells) were obtained from ATCC and cultured as previously reported (Inoue et al., 2001), with or without the following agents: troglitazone (Sankyo, Tokyo, Japan), pioglitazone (Takeda Chemical Industries, Osaka, Japan), 15-deoxy-Δ12,14-prostaglandin J2 (Sigma, St. Louis, MO), which is one of the natural ligands of PPARγ, or 9-*cis*-retinoic acid (Sigma), which is the ligand of the retinoid X receptor.

2.2. Northern blot analysis

Total cellular RNA was isolated from cultured cells using TRIzol reagents (Gibco BRL, Gaithersburg, MD). Northern blot analysis was performed as described elsewhere (Tanaka et al., 1999). The human PPARγ probe consisted of an 858-base pair fragment of the cDNA corresponding to nucleotides 329–1186 of the human PPARγ1 cDNA. The human CCR2 probe consisted of a 939-base pair fragment of the CCR2 cDNA corresponding to nucleotides 1–939. A human β-actin probe (Wako, Japan) was used to monitor the amount of total RNA in each sample.

2.3. Establishment of U937 cells permanently expressing PPARγ

U937 cells permanently expressing PPARγ were established by using the PPARγ expression vector (pCMX-mPPARγ), which contains a cytomegalovirus enhancer and mouse full-length PPARγ cDNA, as we previously reported and explained in detail (Inoue et al., 2001).

2.4. Chemotaxis assay

The cell migration was evaluated with the modified Boyden chamber technique using a 96-well chemotaxis chamber (Neuroprobe, Cabin John, MD) with 50 μl of cell suspension (2×10^7 cells/ml cells in Roswell Park Memorial Institute medium (RPMI)), as previously reported by us (Sawada et al., 2000).

2.5. Equilibrium binding analysis

The cells were suspended at a density of 2×10^7 cells/ml in 200 μl of binding buffer containing 0.1% bovine serum albumin. The cells were incubated with 0.02 nM ^{125}I-MCP-1 and various amounts of unlabelled ligand for 90 min at 25 °C. All assays were done in triplicate, and binding data were examined with the Ligand Assistance Program (Ligand Pharmaceuticals, Charlotte, NC) or Scatchard analysis.

2.6. Balloon angioplasty and troglitazone administration

Homozygous male WHHL rabbits (10 months old, 3.6±0.1 kg) were used for this study. The rabbits were supplied by Sankyo Pharmaceutical. All animals used in the present study were treated with humane care in compliance with the *Guide for the Care and Use of Laboratory Animals* prepared by the National Academy of Sciences and published by the National Institutes of Health (NIH

publication No. 85-23, revised 1985). Each WHHL rabbit was fully anesthetized with sodium pentobarbital (25 mg/kg body weight). A 4F Fogarty balloon catheter was inserted from the left femoral artery, and after the balloon was inflated with air (0.3 ml in the thoracic region and 0.2 ml in the abdominal region), the intima of the thoracic and abdominal aorta was denuded by three passages of the catheter, as we previously reported (Doi et al., 2001). One group (n=8) received troglitazone at a concentration of 100 mg/kg body weight/day from 2 weeks before the angioplasty until 6 weeks after the balloon treatment and the other group (n=8) was given a control solvent. Two rabbits in the control group died during the catheterization and were dropped from the study.

2.7. Pathological examination, immunohistochemical analysis and evaluation of re-endothelialization

The rabbits were fully anesthetized and then killed 6 weeks after the angioplasty. Thirty minutes before they were killed, the animals received an intravenous injection of 6 mL of 0.5% Evans blue dye delivered via the ear vein to identify the remaining non-endothelialized area, as previously described by us (Doi et al., 2001). The area of the intimal surface that was stained blue after the application of Evans blue dye was considered to represent the portion of the arterial segment that remained endothelium deficient. Computerized planimetry (NIH image ver 1.61) was used for analysis. Next, two segments each from the thoracic aorta and the abdominal aorta were obtained from each rabbit (four sites per rabbit). The segments were fixed in methanol–Carnoy's fixative and processed routinely, embedded in paraffin and sectioned into 5-μm-thick slices. The serial sections from each segment were stained with hematoxylin–eosin or with the anti-smooth muscle actin monoclonal antibody (mAb) (1A4; Deckman) or with anti-rabbit macrophage mAb RAM11 (Dako), as we previously reported (Inoue et al., 1998). The acute recruitment or infiltration of macrophages after the angioplasty was evaluated by counting the number of RAM-11$^+$ macrophages on the surface of the aorta (see Fig. 6).

2.8. Reverse transcription-polymerase chain reaction (RT-PCR) for VEGF

The aorta was frozen in liquid N2 immediately after sacrifice and stored at −80 °C until further study. The frozen aorta was homogenized in cold TRIzol reagent (Invitrogen) and total RNA was extracted according to the manufacturer's instructions. cDNA synthesis was performed with 1 μg of total RNA, oligo(dT)20 and ThermoScript (Invitrogen). Incubation lasted for 40 min at 55 °C. The sense primer for rabbit VEGF was 5′GTGGACATCTT CCAGG AGTA-3′and the antisense primer 5′TCTTTGGTCTGCATTCAC A-3′as described previously (Skorjanc et al., 1998). For rabbit G3PDH, the sense primer was 5′ACCACGGTGCACGCCATCAC-3′ and the antisense primer was 5′TCCACCA CCCTGTTGCTGTA-3′ PCR was performed with 2 μL of cDNA template, 2.5U Platinum Taq DNA Polymerase (Invitrogen) and 0.4 μM of the sense and antisense primers. The annealing temperature was 57 °C for VEGF and 60 °C for G3PDH and the number of cycles was 30 for both. Product detection [226 nucleotides for VEGF and 450 for G3PDH] was performed after electrophoresis on 2% agarose gel using ethidium bromide staining.

2.9. Statistical analysis

All values were expressed as mean±S.E.M. Factorial analysis of variance (ANOVA) followed by the Fischer's protected least significant difference test was used to identify significant differences in multiple comparisons.

3. Results

3.1. Induction of PPARγ expression by PPARγ and retinoid X receptor ligands in monocytes/macrophages

PPARγ mRNA was not detected in U937 whether treated or not with PPARγ and retinoid X receptor ligands. While unstimulated THP-1 expressed PPARγ mRNA at a low level, treatment of THP-1 with PPARγ ligands (10^{-5} mol/l troglitazone, 10^{-5} mol/l pioglitazone, or 10^{-5} mol/l 15-deoxy-Δ12,14-prostaglandin J2) or retinoid X receptor ligand (10^{-7} mol/l 9-*cis*-retinoic acid) resulted in a significant increase of PPARγ expression in THP-1. Stimulation with a combination of troglitazone and 9-*cis*-retinoic acid resulted in further up-regulation of PPARγ mRNA expression (Fig. 1).

3.2. Inhibition of proliferation of THP-1 by PPARγ and retinoid X receptor ligands

Cells (1.0×10^5 cells/ml) were cultured for 5 days in the presence of various doses of one of the thiazolidinediones, 15-deoxy-Δ12,14-prostaglandin J2, 9-*cis*-retinoic acid or combination thereof. When cells were treated with vehicle alone, the number of cells significantly increased 7.2 times after 5 days in culture. Troglitazone, pioglitazone, 15-deoxy-Δ12,14-prostaglandin J2 or 9-*cis*-retinoic acid caused a concentration-dependent suppression of cell growth. With 10^{-5} mol/l troglitazone, pioglitazone, 15-deoxy-Δ12,14-prostaglandin J2 and 10^{-7} mol/l 9-*cis*-retinoic acid alone, cell proliferation was inhibited by 60%, 51%, 56% and 39%, respectively, after 5 days. The simultaneous treatment of cells with both 10^{-5} mol/l troglitazone and 10^{-7} mol/l 9-*cis*-retinoic acid produced a 77% inhibition of cell growth. No effect was observed with troglitazone (10^{-5} mol/l) when used alone or in combination with 9-*cis*-retinoic acid (10^{-7} mol/l) in U937 cells in which PPARγ was not detected.

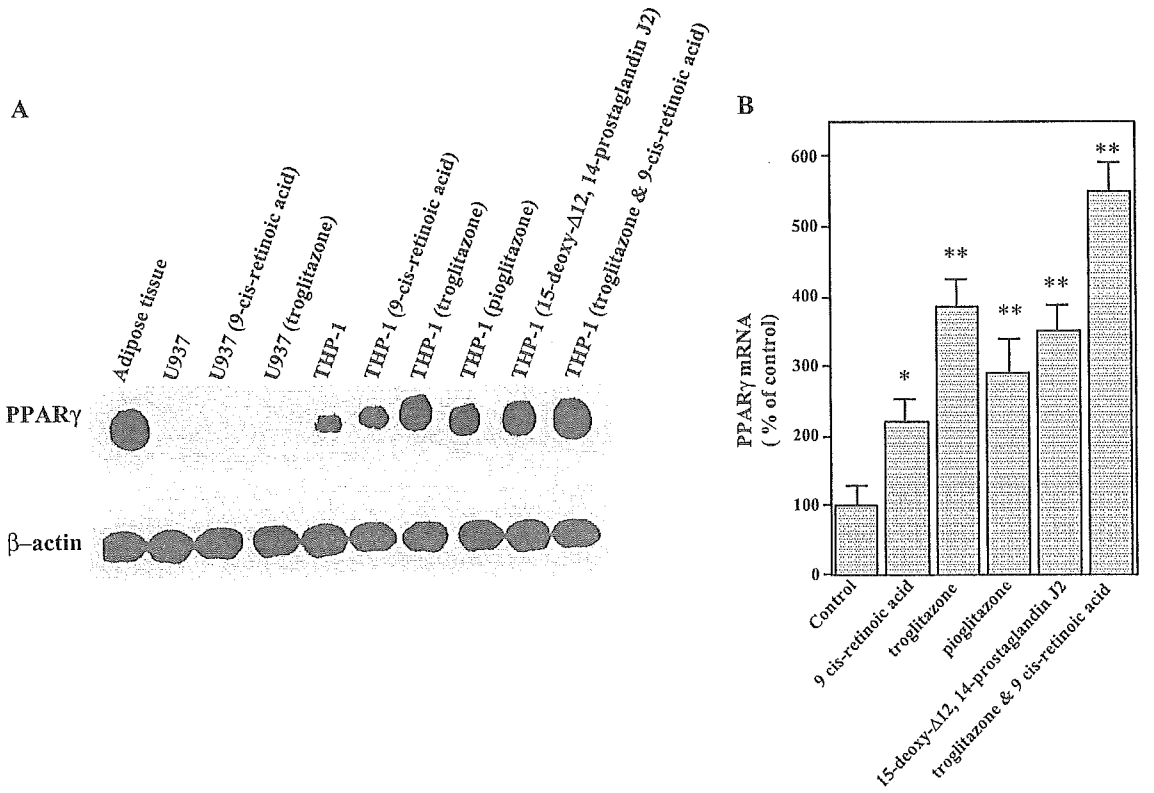

Fig. 1. Induction of PPARγ mRNA expression by PPARγ and retinoid X receptor ligands in monocytes/macrophages. U937 and THP-1 were incubated with 10^{-5} mol/l of troglitazone, pioglitazone, and 15-deoxy-Δ12,14-prostaglandin J2 and with 10^{-7} mol/l of 9-*cis*-retinoic acid for 24 h and their effects on PPARγ mRNA expression were evaluated by Northern blot analysis. (A) Northern blot analysis of PPARγ mRNA in adipose tissue, U937, and THP-1. Twenty micrograms of total RNA per lane were used for the analysis. (B) Quantitative measurements of PPARγ mRNA levels in THP-1. $*P<0.05$ and $**P<0.01$ vs. corresponding controls (n=4).

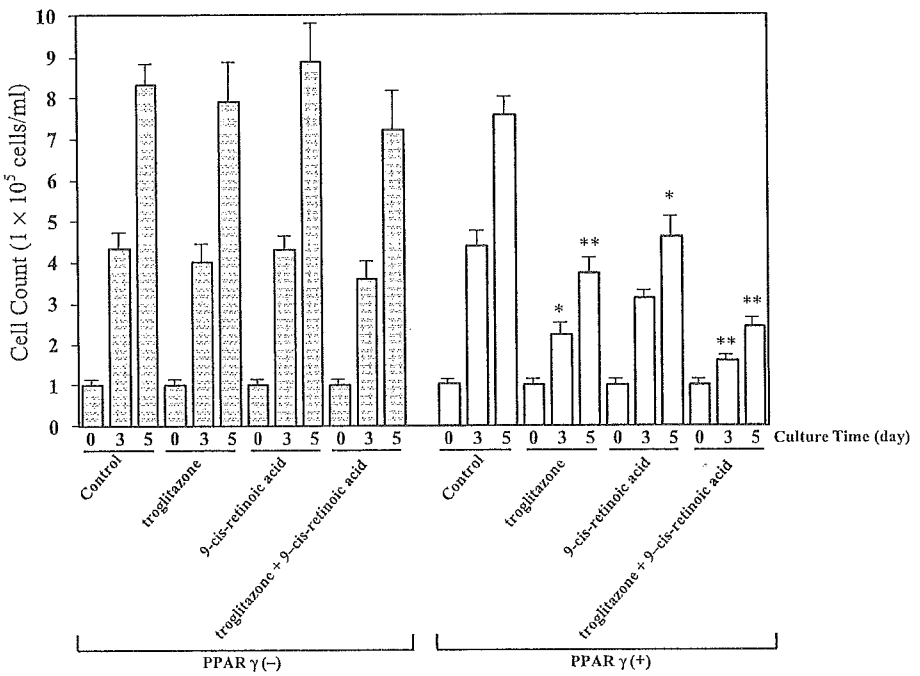

Fig. 2. Inhibition of proliferation of U937 cell expressing PPARγ by troglitazone and 9-*cis*-retinoic acid. Wild-type U937 cells and U937 cells stably transfected with PPARγ expression vector were plated at 1.0×10^5 cells/ml and cultured for 5 days in the presence of 10^{-5} mol/l of troglitazone and 10^{-7} mol/l of 9-*cis*-retinoic acid alone or in combination. Cell numbers were counted after 3 and 5 days. $*P<0.05$ and $**P<0.01$ vs. corresponding controls (n=4).

3.3. Restoration of responsiveness to troglitazone and 9-cis RA in U937 expressing PPARγ

To further characterize the role of PPARγ in monocytes/macrophages proliferation, we utilized the permanent cell line of U937 expressing PPARγ. As shown in Fig. 2, troglitazone or 9-*cis*-retinoic acid treatment of these cell lines resulted in a marked inhibition of cell growth, similar to that of THP-1. With 10^{-5} mol/l of troglitazone alone, cell proliferation was inhibited by 56% after 5 days, and with 10^{-7} mol/l 9-*cis*-retinoic acid alone by 45%. Moreover, treatment of the cells with a combination of 10^{-5} mol/l troglitazone and 10^{-7} mol/l 9-*cis*-retinoic acid resulted in a 71% inhibition of cell growth (Fig. 2).

3.4. Inhibition of MCP-1-induced migration of THP-1 by PPARγ and retinoic X receptor ligands

The chemotactic response of THP-1 to MCP-1, troglitazone, 15-deoxy-Δ12,14-prostaglandin J2 and 9-*cis*-retinoic acid was assessed during a 2-h incubation. The treatment with MCP-1 resulted in a dose-dependent induction in the migration of THP-1 (5 To 50 ng/ml), but THP-1 cells did not show a significant migratory response to troglitazone, 15-deoxy-Δ12,14-prostaglandin J2 or 9-*cis*-retinoic acid. Pretreatment with troglitazone for 24 h significantly inhibited the migration of THP-1 induced by MCP-1 (25 ng/ml), and with 10^{-7} mol/l troglitazone, the migration of THP-1 was inhibited by 44%. Maximal inhibition (66%, $P<0.01$) of THP-1 migration was observed in response to treatment with 10^{-4} mol/l troglitazone (Fig. 3A). Pretreatment with 15-deoxy-Δ12,14-prostaglandin J2 or 9-*cis*-retinoic acid also inhibited the migration of THP-1 under the same conditions (Fig. 3B,C), while troglitazone and 9-*cis*-retinoic acid (10^{-7} mol/l) had an even more profound inhibitory effect on migration (Fig. 3D).

3.5. Regulation of CCR2 mRNA expression by troglitazone, 15-deoxy-Δ12,14-prostaglandin J2 and 9-cis RA In THP-1

We also examined the effect of troglitazone, 15-deoxy-Δ12,14-prostaglandin J2 and 9-*cis*-retinoic acid on CCR2

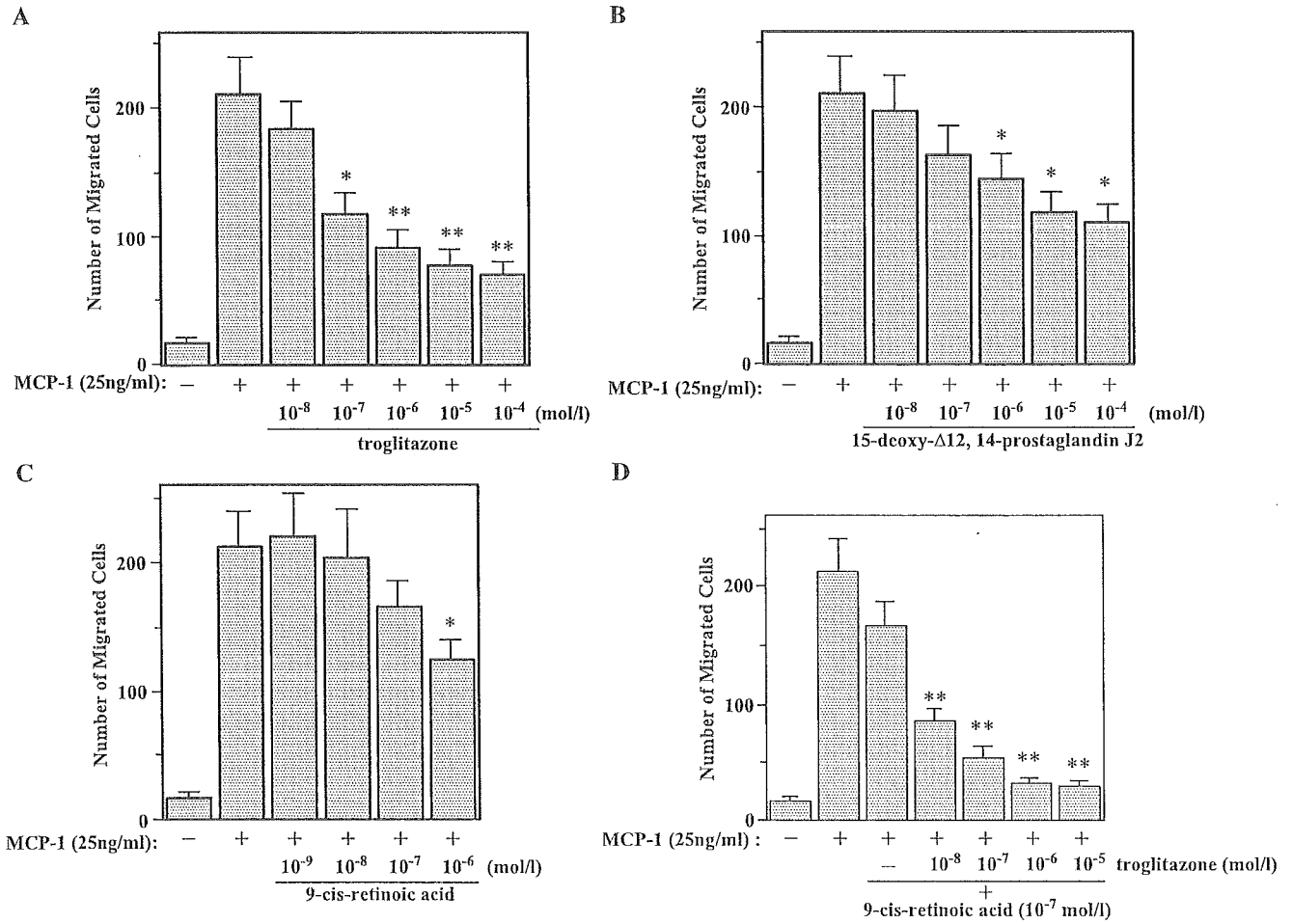

Fig. 3. Inhibition of MCP-1-induced migration of THP-1 by PPARγ and retinoid X receptor ligands. THP-1 were pretreated with different concentrations of troglitazone (A), 15-deoxy-Δ12,14-prostaglandin J2 (B), 9-*cis*-retinoic acid (C) alone or in combination with troglitazone and 9-*cis*-retinoic acid (D) for 24 h at 37 °C. MCP-1 (25 ng/ml) was added to the lower wells as the chemoattractant and 2 h migration assays were performed ($n=6$). *$P<0.05$ and **$P<0.01$ vs. 25 ng/ml of MCP-1 alone.

expression. treatment with 10^{-5} mol/l troglitazone resulted in a time-dependent reduction in the expression of CCR2 mRNA. The inhibitory effect of 10^{-5} mol/l of troglitazone was first observed after a 6-h incubation and persisted for at least a 48-h exposure (Fig. 4A). Treatment with troglitazone (10^{-7} mol/l to 10^{-4} mol/l) suppressed CCR2 mRNA expression in a dose-dependent fashion (Fig. 4B,C). The maximum decrease of 93% occurred in response to 10^{-4} mol/l of troglitazone. Treatment with 15-deoxy-Δ12,14-prostaglandin J2 (10^{-6}–10^{-4} mol/l) and with 9-*cis*-retinoic acid (10^{-7}–10^{-6} mol/l) also suppressed the CCR2 mRNA level in a dose-dependent fashion (Fig. 4B,C).

To determine whether the down-regulation of CCR2 is a transcriptional or post-transcriptional event, we analyzed the effect of troglitazone on the expression of CCR2 mRNA in the presence of actinomycin D (3 μg/ml, Sigma), a transcriptional inhibitor. When treated with actinomycin D, a linear decrease in the level of CCR2 mRNA without the treatment of troglitazone was observed (T1/2; 3 h). With the treatment of troglitazone, the level of CCR2 mRNA also

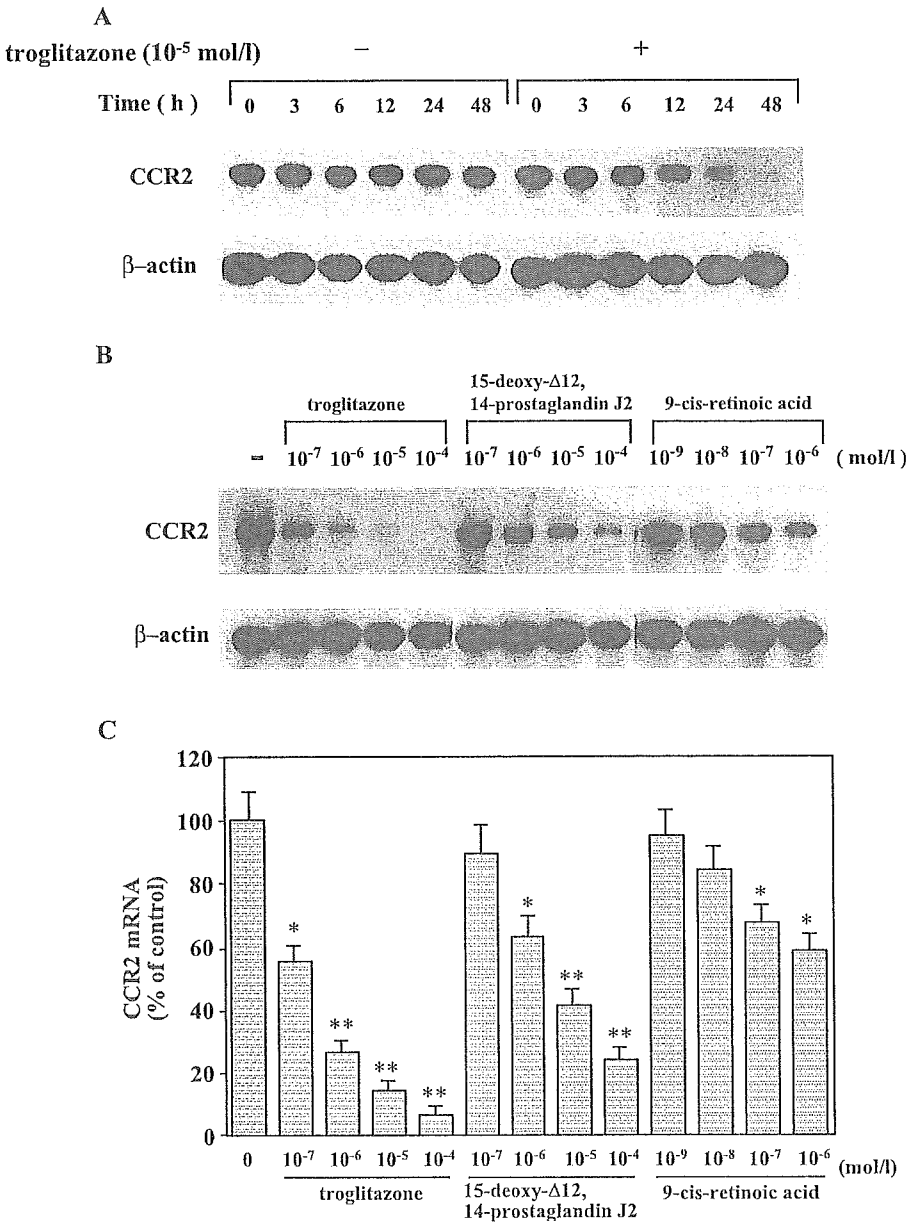

Fig. 4. Regulation of CCR2 mRNA expression by troglitazone, 15-deoxy-Δ12,14-prostaglandin J2 or 9-*cis*-retinoic acid in THP-1. (A) Time-dependent effect of troglitazone on CCR2 mRNA expression. THP-1 cells were incubated with or without 10^{-5} mol/l of troglitazone and harvested after various incubation times for RNA isolation. Twenty micrograms of total RNA per lane was used for the analysis. Similar results were obtained in three independent experiments. (B) Concentration-dependent effect of troglitazone, 15-deoxy-Δ12,14-prostaglandin J2 and 9-*cis*-retinoic acid on CCR2 mRNA expression. THP-1 were incubated with or without various concentrations of troglitazone, 15-deoxy-Δ12,14-prostaglandin J2 and 9-*cis*-retinoic acid harvested 24 h after incubation. Twenty micrograms of total RNA per lane was used for the analysis. (C) Quantitative measurements of CCR2 mRNA levels after administration of troglitazone, 15-deoxy-Δ12,14-prostaglandin J2, or 9-*cis*-retinoic acid. $^{*}P<0.05$ and $^{**}P<0.01$ vs. corresponding controls ($n=4$).

decreased, but at a similar rate to that of the control not treated with troglitazone (Fig. 5A,B).

3.6. Inhibition of MCP-1 binding to THP-1 by troglitazone and 9-cis RA

Under the same experimental condition as described above, we also examined the effects of troglitazone on the binding of MCP-1 to THP-1. THP-1 was pretreated for 24 h with or without 10^{-5} mol/l of troglitazone. As illustrated in Fig. 6A, Scatchard analysis showed that K_d values were similar for the control and troglitazone-treated groups (0.61±0.13 nmol/l for the control and 0.65±0.16 nmol/l for the troglitazone-treated group). In contrast, the troglitazone-treated THP-1 expressed 4.3±0.8 fmol of receptors/10^6 cells, while the control THP-1 expressed 11.7±1.6 fmol/10^6 cells. Thus, troglitazone (10^{-5} mol/l) reduced the number of MCP-1 receptor on the cell surface by 64%. Fig. 6B shows the time course of the effect of troglitazone and 9-*cis*-retinoic acid on the binding of MCP-1 to THP-1. At 10^{-5} mol/l of troglitazone alone, the binding was inhibited by 51% after 12 h and by 66% after 24 h, and the simultaneous treatment of cells with 10^{-5} mol/l troglitazone and 10^{-7} mol/l 9-*cis*-retinoic acid resulted in 85% inhibition.

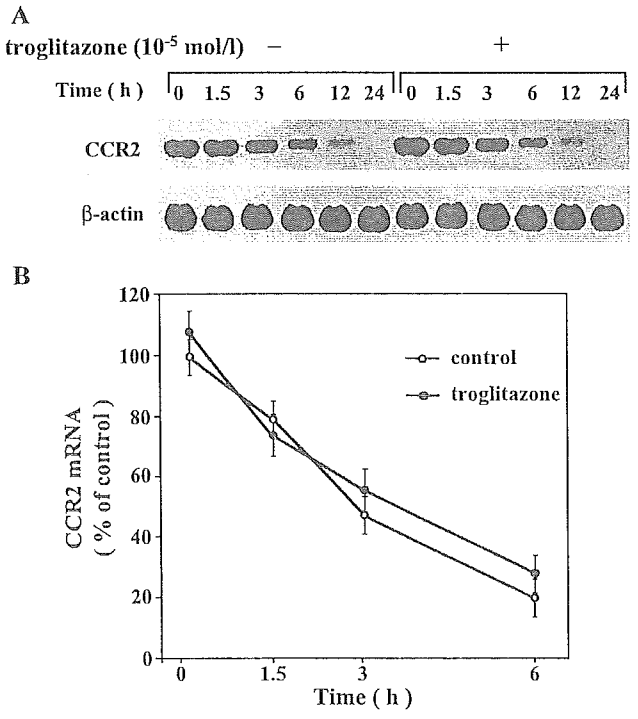

Fig. 5. Effect of troglitazone on the expression of CCR2 mRNA in the presence of actinomycin D. (A) THP-1 were incubated with 3 μg/ml of actinomycin D with or without 10^{-5} mol/l of troglitazone for 24 h and harvested after various incubation times for RNA isolation. Twenty micrograms of total RNA per lane was used for the analysis. (B) Quantitative measurements of CCR2 mRNA levels after treatment with 3 μg/ml of actinomycin D with or without 10^{-5} mol/l of troglitazone (n=3).

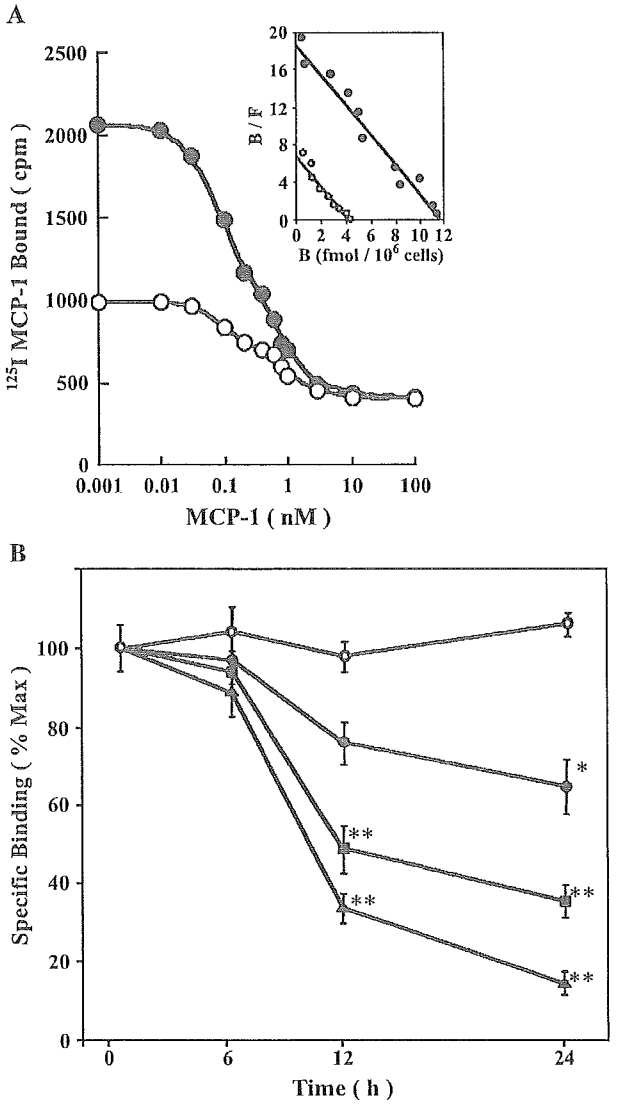

Fig. 6. Inhibition of MCP-1 binding to THP-1 by troglitazone and 9-*cis*-retinoic acid. (A) ^{125}I-labelled MCP-1 binding curve and Scatchard plot analysis. THP-1 were pretreated with (white circles) or without (black circles) 10^{-5} mol/l of troglitazone for 24 h at 37 °C. Insets show Scatchard analysis of the specific binding data. The results are representative of three independent experiments. (B) Time course of troglitazone and 9-*cis*-retinoic acid-induced reduction of MCP-1 binding to THP-1. The cells were incubated for up to 24 h at 37 °C without treatment (white circle) or with 10^{-5} M of troglitazone (black square) or 10^{-7} mol/l of 9-*cis*-retinoic acid (black circle) alone or in combination (black triangle). The binding of ^{125}I-MCP-1 was determined in the presence or absence of 100 nmol/l of unlabeled MCP-1. *P<0.05 and **P<0.01 vs. corresponding controls.

3.7. Suppression by troglitazone of monocyte and macrophage recruitment onto the balloon-injured aorta of WHHL rabbits

At the end of the study, 10-month-old WHHL rabbits belonging to the control group exhibited severe atherosclerotic lesions in thoracic aortae (61±11% of the total surface area) and patchy lesions in abdominal aortae (37±9%). Treatment with troglitazone for a total of 8 weeks did not

noticeably change the gross appearance of the atherosclerotic lesions (66±8% in thoracic aortae and 32±7% in abdominal aortae). The immunohistochemical analysis showed that the troglitazone treatment had no significant effect on the total content of $1A4^+$ vascular smooth muscle cells (1A4-positive area/atheromatous area: 11.4±3.9% in

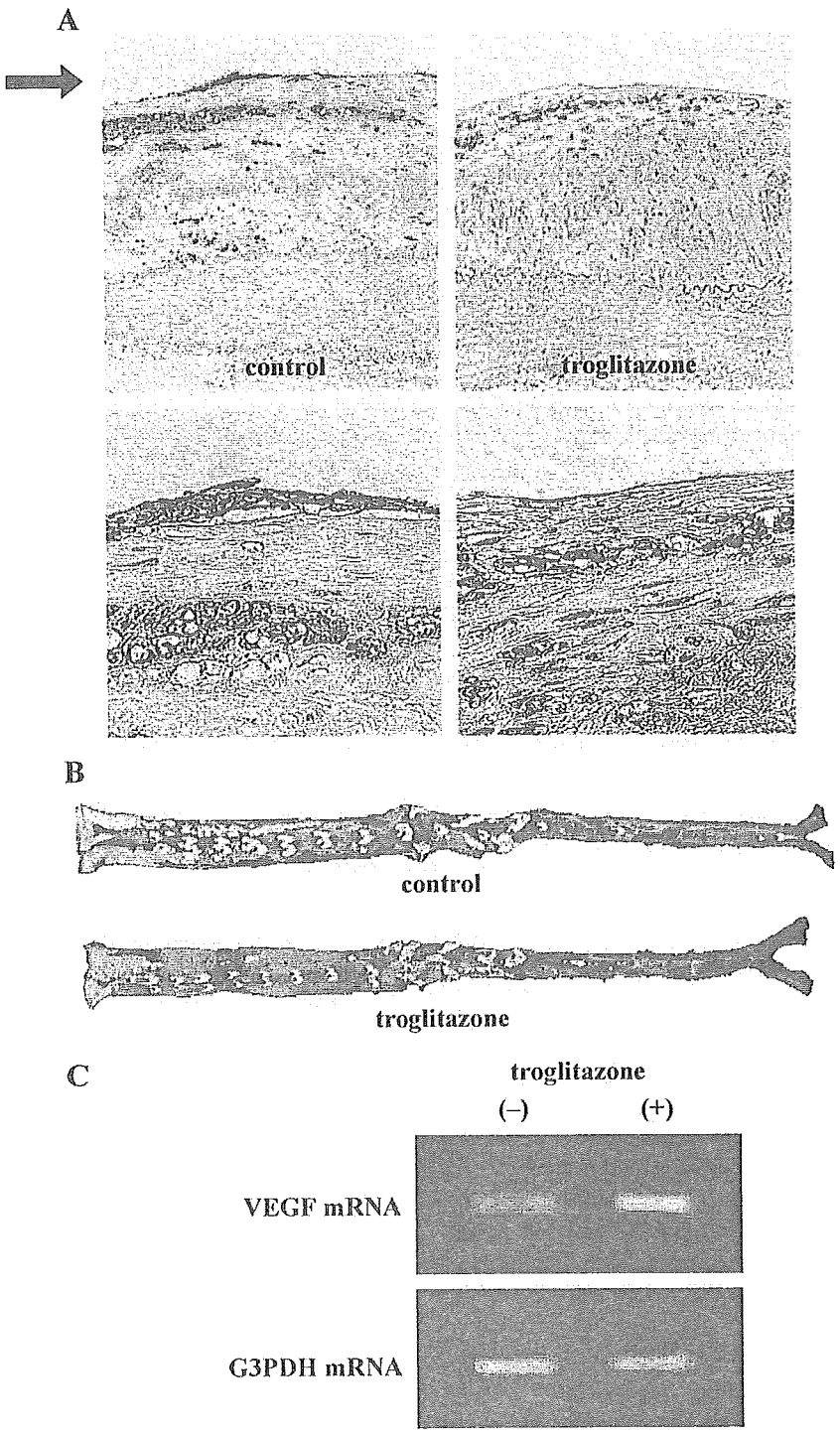

Fig. 7. Effect of troglitazone administration to balloon-injured WHHL rabbits. (A) Suppression of recruitment of monocytes/macrophages onto the surface of the aorta of WHHL rabbits 6 weeks after balloon injury. Troglitazone was administered every day for 8 weeks, from 2 weeks before injury until sampling. RAM11-positive immunostaining shows monocytes/macrophages in brown. Top: Lower magnification of the whole blood vessel. Bottom: Higher magnification of the surface of the balloon-injured aortas (the portion indicated by arrow in top). (B) Macroscopic appearance of balloon-injured aortas of WHHL rabbits after the injury. Area of re-endothelialization is not stained by Evans blue dye and appears white. Control: vehicle-treated group; troglitazone: troglitazone-treated group. (C) Analysis of VEGF gene expression. Pooled frozen aortic samples (vehicle-treated group: n=6; troglitazone-treated group: n=8) were subjected to RT-PCR for VEGF.

the abdominal and 9.3±1.1% in the thoracic aortae of the control group; 6.3±0.7% in the abdominal and 7.8±1.7% in the thoracic aortae of the troglitazone-treated group), although there was a tendency for the vascular smooth muscle cell content to decrease as a result of the troglitazone treatment, which is compatible with the results of previous studies with different experimental protocols (Shiomi et al., 1999; Law et al., 1996). Nor did the treatment significantly affect the total content of $RAM11^+$ monocytes/macrophages (RAM11-positive area/atheromatous area: 11.6±3.7% in the thoracic and 14.3±4.8% in the abdominal aortae of the control group; 14.9±3.1% in the thoracic and 12.8±2.5% in the abdominal aortae of the troglitazone-treated group).

However, the number of acutely recruited monocytes/macrophages onto the surface of the balloon injured aorta was significantly lower in the abdominal aorta of the troglitazone-treated group (39±5% of the control, $P<0.05$), although in the thoracic aorta of this group the reduction in numbers did not reach statistical significance (82±7% of the control) (Fig. 7A).

3.8. Re-endothelialization in balloon-injured aorta of WHHL rabbits accelerated by troglitazone

Evans blue staining demonstrated that the denuded area was significantly smaller in the aorta of the troglitazone-treated group than of the control group (Fig. 7B; Evans blue-stained area/non-atheromatous area: 0.4±0.2% for the troglitazone-treated and 4.8±1.2% for the control group; $P<0.05$). RT-PCR for VEGF showed that VEGF gene expression had increased in the aorta of the troglitazone-treated group (Fig. 7C).

4. Discussion

The study presented here demonstrated that PPARγ and retinoid X receptor ligands caused a concentration-dependent suppression of cell growth in PPARγ-expressing THP-1 cells. In contrast, troglitazone and 9-*cis*-retinoic acid had no effect on the proliferation of wild-type U937 which lack PPARγ expression. We further demonstrated that U937 cell lines with stable PPARγ expression restored the responsiveness to troglitazone and 9-*cis*-retinoic acid for growth suppression. These findings indicate that activation of PPARγ in monocytes/macrophages causes growth suppression of these cell lines.

We could also demonstrate that PPARγ and retinoid X receptor specific ligands strongly inhibited the MCP-1-induced migration of THP-1. This result is compatible with those reported in previous publications (Zhu et al., 1999; Kintscher et al., 2000). To investigate the potential mechanism of inhibition of MCP-1-induced migration by PPARγ activation, we also examined changes in the functional expression of CCR2 in THP-1. We found that troglitazone, 15-deoxy-Δ12,14-prostaglandin J2 and 9-*cis*-retinoic acid had a strong down-regulatory effect on CCR2 mRNA expression at the transcriptional level. We further confirmed that MCP-1 binding activity was also reduced and the number of MCP-1 receptors (CCR2) declined as a result of exposure to troglitazone and 9-*cis*-retinoic acid. Since it has been reported that in an in vitro chemotaxis assay, monocytes derived from CCR2 knockout mice failed to migrate in response to MCP-1 (Boring et al., 1997), the suppressive action of PPARγ and retinoid X receptor ligands on MCP-1-induced migration can be interpreted as representing the down-regulation of CCR2 expression.

Other studies have demonstrated that CCR2 or MCP-1 knockout mice are less susceptible to atherosclerosis and showed low monocyte recruitment in vascular lesions (Boring et al., 1998; Gu et al., 1998). The potent suppressive action of PPARγ and retinoid X receptor ligands on MCP-1-induced migration of THP-1 observed in our study suggests therefore the protective role of PPARγ in the development of atherosclerosis.

We also investigated in vivo the therapeutic effectiveness of troglitazone on acute recruitment of monocytes/macrophages onto the atheromatous lesion after balloon injury in WHHL rabbits. Since we utilized 10-month-old WHHL rabbits with fully developed atherosclerosis to examine the effect of troglitazone on the acute recruitment of monocytes onto atheromatous lesions, the effect of troglitazone on pre-existing atheromas was not as prominent as that reported by another study, which examined the effect of troglitazone on the development of atherosclerosis in younger WHHL rabbits (Shiomi et al., 1999). However, compatible with the in vitro effect of thiazolidinediones on monocytes/macrophages observed in our study, we also found in vivo evidence of suppression of acute adhesion and/or subsequent transendothelial migration in response to troglitazone treatment. Han et al. (2000) recently showed that oxLDL reduces circulating monocyte CCR2 expression through activation of PPARγ and postulated that oxLDL may promote the arrest of newly recruited monocytes in the arterial wall. However, our findings contradict their hypothesis, that is, the administration of the PPARγ agonist suppressed attachment and/or proliferation of monocytes/macrophages on atherosclerotic lesions at the site of balloon injury.

A previous study of ours found that thiazolidinediones stimulate endothelial proliferation and induce regeneration in vitro within clinically relevant doses (Fukunaga et al., 2001). The significant acceleration of re-endothelialization in the aorta after balloon injury observed in the study presented here was thus highly compatible with our previous in vitro findings. Accelerated re-endothelialization may be ascribed to the enhanced expression of pro-angiogenic factors previously demonstrated by us (Inoue et al., 2001; Itoh et al., 1999). In fact, troglitazone administration used in the current study showed increased gene expression of VEGF in the aorta of the WHHL rabbits.

In conclusion, we showed that PPARγ and retinoid X receptor specific ligands inhibited proliferation and migration of monocytes/macrophages as well as suppressed the functional expression of the MCP-1 receptor, CCR2 in THP-1. The administration of thiazolidinediones to WHHL rabbits inhibited monocyte/macrophage recruitment and induced endothelial regeneration after balloon injury. These results indicate the involvement of PPARγ in modulating monocyte proliferation, recruitment and transmigration through the endothelial cell layers under various pathological conditions and suggest the therapeutic potential of thiazolidinediones for diabetic vascular complications, which has been implied by some human studies (Minamikawa et al., 1998).

Acknowledgements

This work was supported in part by research grants from the Japanese Ministry of Education, Science and Culture, the Japanese Society for the Promotion of Science's 'Research for the Future' program (JSPS-RFTF 96100204, JSPS-RFTF 98L00801), and the Japan Smoking Research Foundation.

References

Boring, L., Gosling, J., Chensue, S.W., Kunkel, S.L., Farese Jr., R.V., Broxmeyer, H.E., Charo, I.F., 1997. Impaired monocyte migration and reduced type 1 (Th1) cytokine responses in C-C chemokine receptor 2 knockout mice. J. Clin. Invest. 100, 2552–2561.

Boring, L., Gosling, J., Cleary, M., Charo, I.F., 1998. Decreased lesion formation in CCR2−/− mice reveals a role for chemokines in the initiation of atherosclerosis. Nature 394, 894–897.

Charo, I.F., Myers, S.J., Herman, A., Franci, C., Connolly, A.J., Coughlin, S.R., 1994. Molecular cloning and functional expression of two monocyte chemoattractant protein-1 receptors reveals alternative splicing of the carboxyl-terminal tails. Proc. Natl. Acad. Sci. U. S. A. 191, 2752–2756.

Chen, Z., Ishibashi, S., Perrey, S., Osuga, J., Gotoda, T., Kitamine, T., Tamura, Y., Okazaki, H., Yahagi, N., Iizuka, Y., Shionoiri, F., Ohashi, K., Harada, K., Shimano, H., Nagai, R., Yamada, N., 2001. Troglitazone inhibits atherosclerosis in apolipoprotein E-knockout mice. Arterioscler. Thromb. Vasc. Biol. 21, 372–377.

Collins, A.R., Meehan, W.P., Kintscher, U., Jackson, S., Wakino, S., Noh, G., Palinski, W., Hsueh, W.A., Law, R.E., 2001. Troglitazone inhibits formation of early atherosclerotic lesions in diabetic and nondiabetic low density lipoprotein receptor-deficient mice. Arterioscler. Thromb. Vasc. Biol. 21, 365–371.

DeFronzo, R.A., Ferrannini, E., 1991. Insulin resistance: a multifaceted syndrome responsible for NIDDM, obesity, hypertension, dyslipidemia and atherosclerotic cardiovascular disease. Diabetes Care 14, 173–194.

Doi, K., Ikeda, T., Itoh, H., Ueyama, K., Hosoda, K., Ogawa, Y., Yamashita, J., Chun, T.-H., Inoue, M., Masatsugu, K., Sawada, N., Fukunaga, Y., Saito, T., Sone, M., Yamahara, K., Kook, H., Komeda, M., Ueda, M., Nakao, K., 2001. C-type natriuretic peptide induces redifferentiation of vascular smooth muscle cells with accelerated reendothelialization. Arterioscler. Thromb. Vasc. Biol. 21, 930–936.

Fukunaga, Y., Itoh, H., Doi, K., Tanaka, T., Yamashita, J., Chun, T.-H., Inoue, M., Masatsugu, K., Sawada, N., Saito, T., Hosoda, K., Kook, H., Ueda, M., Nakao, K., 2001. Thiazolidinediones, peroxisome proliferator-activated receptor γ agonists, regulate endothelial cell growth and secretion of vasoactive peptides. Atherosclerosis 158, 113–119.

Gu, L., Okada, Y., Clinton, S.K., Gerard, C., Sukhova, G.K., Libby, P., Rollins, B.J., 1998. Absence of monocyte chemoattractant protein-1 reduces atherosclerosis in low density lipoprotein receptor-deficient mice. Mol. Cell 2, 275–281.

Han, K.H., Chang, M.K., Boullier, A., Green, S.R., Li, A., Glass, C.K., Quenhenberger, O., 2000. Oxidized LDL reduces monocyte CCR2 expression through pathways involving peroxisome proliferator-activated receptor-γ. J. Clin. Invest. 106, 793–802.

Inoue, M., Itoh, H., Ueda, M., Naruko, T., Kojima, A., Komatsu, R., Doi, K., Ogawa, Y., Tamura, N., Takaya, K., Igaki, T., Yamashita, J., Chun, T.-H., Masatsugu, K., Becker, A.E., Nakao, K., 1998. Vascular endothelial growth factor (VEGF) expression in human coronary atherosclerotic lesions: possible pathophysiological significance of VEGF in progression of atherosclerosis. Circulation 98, 2108–2116.

Inoue, M., Itoh, H., Tanaka, T., Chun, T.-H., Doi, K., Fukunaga, Y., Sawada, N., Yamashita, J., Masatsugu, K., Saito, T., Sakaguchi, S., Sone, M., Yamahara, K., Yurugi, T., Nakao, K., 2001. Oxidized low density lipoprotein regulates VEGF expression in human macrophages and endothelial cells through activation of PPARγ. Arterioscler. Thromb. Vasc. Biol. 21, 560–566.

Itoh, H., Doi, K., Tanaka, T., Fukunaga, Y., Hosoda, K., Inoue, G., Nishimura, H., Yoshimasa, Y., Yamori, Y., Nakao, K., 1999. Hypertension and insulin resistance—the role of peroxisome proliferator-activated receptor-γ. Clin. Exp. Pharmacol. Physiol. 26, 558–560.

Kintscher, U., Goetze, S., Wakino, S., Kim, S., Nagpal, S., Chandraratna, R.A.S., Graf, K., Fleck, E., Hsueh, W.A., Law, R.E., 2000. Peroxisome proliferator-activated receptor and retinoid X receptor ligands inhibit monocyte chemotactic protein-1-directed migration of monocytes. Eur. J. Pharmacol. 401, 259–270.

Law, R.E., Meehan, W.P., Xi, X.-P., Graf, K., Wuthrich, D.A., Coats, W., Faxon, D., Hsueh, W.A., 1996. Troglitazone inhibits vascular smooth muscle cell growth and intimal hyperplasia. J. Clin. Invest. 98, 1897–1905.

Lehmann, J.M., Moore, L.B., Smith-Oliver, T.A., Wilkinson, W.O., Willson, T.M., Kliewer, S.A., 1995. An antidiabetic thiazolidinedione is a high affinity ligand for peroxisome proliferator-activated receptor gamma (PPAR gamma). J. Biol. Chem. 270, 12953–12956.

Minamikawa, J., Tanaka, S., Yamauchi, M., Inoue, D., Koshiyama, H., 1998. Potent inhibitory effect of troglitazone on carotid arterial wall thickness in type 2 diabetes. J. Clin. Endocrinol. Metab. 83, 1818–1820.

Nagy, L., Tontonoz, P., Alvarez, J.G.A., Chen, H., Evans, R.M., 1998. Oxidized LDL regulates macrophage gene expression through ligand activation of PPARgamma. Cell 93, 229–240.

Nelken, N.A., Coughlin, S.R., Gordon, D., Wilcox, J.N., 1991. Monocyte chemoattractant protein-1 in human atheromatous plaques. J. Clin. Invest. 88, 1121–1127.

Nolan, J.J., Ludvik, B., Beerdsen, P., Joyce, M., Olefsky, J., 1994. Improvement in glucose tolerance and insulin resistance in obese subjects treated with troglitazone. N. Engl. J. Med. 331, 1188–1193.

Ricote, M., Li, A.C., Willson, T.M., Kelly, C.J., Glass, C.K., 1998. The peroxisome proliferator-activated receptor-gamma is a negative regulator of macrophage activation. Nature 391, 79–82.

Sawada, N., Itoh, H., Ueyama, K., Yamashita, J., Doi, K., Chun, T.-H., Inoue, M., Masatsugu, K., Saito, T., Fukunaga, Y., Sakaguchi, S., Arai, H., Ohno, N., Komeda, M., Nakao, K., 2000. Inhibition of Rho-associated kinase results in suppression of neointimal formation of balloon-injured arteries. Circulation 101, 2030–2033.

Shiomi, M., Ito, T., Tsukada, T., Tsujita, Y., Horikoshi, H., 1999. Combination treatment with troglitazone, an insulin action enhancer, and pravastatin, an inhibitor of HMG-CoA reductase, shows a synergistic effect on atherosclerosis of WHHL rabbits. Atherosclerosis 142, 345–353.

Skorjanc, D., Jaschinski, F., Heine, G., Pette, D., 1998. Sequential increases in capillarization and mitochondrial enzymes in low-frequency-stimulated rabbit muscle. Am. J. Physiol. 274, C810–C818.

Tanaka, T., Itoh, H., Doi, K., Fukunaga, Y., Hosoda, K., Shintani, M., Yamashita, J., Chun, T.-H., Inoue, M., Masatsugu, K., Sawada, N., Saito, T., Inoue, G., Nishimura, H., Yoshimasa, Y., Nakao, K., 1999. Down regulation of peroxisome proliferator-activated receptor gamma expression by inflammatory cytokines and its reversal by thiazolidinediones. Diabetologia 42, 702–710.

Tontonoz, P., Hu, E., Spiegelman, B.M., 1994. Stimulation of adipogenesis in fibroblasts by PPAR gamma 2, a lipid-activated transcription factor. Cell 79, 1147–1156.

Tontonoz, P., Nagy, L., Alvarez, J.G.A., Thomazy, V.A., Evans, R.M., 1998. PPARgamma promotes monocyte/macrophage differentiation and uptake of oxidized LDL. Cell 93, 241–252.

Zhu, L., Bisgaier, C.L., Aviram, M., Newton, R.S., 1999. 9-*Cis* retinoic acid induces monocytes chemoattractant protein-1 secretion in human monocytic THP-1 cells. Arterioscler. Thromb. Vasc. Biol. 19, 2105–2111.